Global Optimization of Pt-Cu Clusters Using a Genetic Algorithm and Density Functional Theory

By

Ezgi ERDEM

A Dissertation Submitted to the Graduate School of Sciences and Engineering in Partial Fulfillment of the Requirements for the Degree of

Master of Science

in

Chemical and Biological Engineering

KOÇ UNIVERSITY

Aug 8, 2017

Global Optimization of Pt-Cu Clusters Using a Genetic Algorithm and Density Functional Theory

Koç University

Graduate School of Sciences and Engineering

This is to certify that I have examined this copy of a master's thesis by

Ezgi Erdem

and have found that it is complete and satisfactory in all respects, and that any and all revisions required by the final examining committee have been made.

Committee Members:

_____

Can Erkey, Ph.D. (Advisor)

_____

Ersin Yurtsever, Ph. D.

_____

Ramazan Yıldırım, Ph.D.

Date: Aug 8, 2017

Dedicated to my beloved family.

ABSTRACT

The atomic arrangements and structures of monometallic Pt and Cu clusters and bimetallic PtCu clusters composed of 2-40 atoms were determined using a genetic algorithm (GA) with multiple runs between 100 and 400. GA was designed associated with the Gupta potential energy with the aim to define atomic interactions within cluster regime. The algorithm was developed and implemented in MATLAB [1] environment. After a large number of GA runs on Pt, Cu and PtCu clusters, the algorithm successfully found the minimum energy structures. To improve our understanding of the structural and energetic properties of the mono- and bimetallic Pt-Cu clusters, a wide range of energetic and structural properties (i.e., excess, binding energy and second difference in energy, effective coordination number, average weighted bond length, and second order parameter) were calculated. Energetic analysis provide strong evidence that the lowest energy structures of Pt, Cu and PtCu clusters were stable and energetically favorable. The optimum structures for every size of Pt and Cu clusters were symmetric, regular and mainly based on icosahedron structures while PtCu clusters above 20 atoms were distorted. The lowest energy structures of PtCu clusters were found as mixed distorted icosahedrons with Pt segregation in core region whereas Cu atoms were located on the surface. Remarkably, 38 atoms of Pt, Cu and PtCu alloy clusters tend to be perfect truncated octahedron which was the similar face centered cubic packing as in bulk Pt and Cu.

Further, global optimization of each composition of 10 atoms of PtCu clusters were carried out with DFT approach using Gaussian 09. Energetically the lowest energy composition was obtained as Pt_3Cu_7. Hydrogen and OH adsorption was studied to investigate how hydrogen interacts with Pt−Cu clusters for improving our understanding of the factors determining the reactivity. Hydrogen and OH adsorption energy and

adsorption properties were found in the different charge states and in different adsorption sites as top, bridge and hollow of Pt_{10}, Cu_{10} and Pt_3Cu_7 clusters. More negative adsorption energy indicates the stronger the adsorption since the adsorption energy measures the magnitude of the binding energy of the species to the cluster. Based on our calculations, the lowest energy structures for H and OH adsorbed on Pt_3Cu_7 cluster were reached in the neutral state. The most favorable adsorption site of hydrogen was found as the top site for Pt_{10} and bridge site for Cu_{10} cluster. For the case of bimetallic Pt_3Cu_7 cluster, the hollow site are more favorable for hydrogen adsorption but Pt-hollow site is more energetically favorable. This result indicates that H atoms show a preference for Pt atoms rather than Cu in Pt_3Cu_7 cluster.

ÖZET

Bu çalışmada Pt, Cu ve PtCu sistemlerinin 2 ila 40 atom aralığında değişen küçük ölçekte kümelerinin sahip olduğu en düşük enerjili morfolojilerin bulunması çalışılmıştır. Yapıların optimizasyonu için yarı-ampirik olan Gupta potansiyeli temel alınmış ve MATLAB ortamında geliştirilen Genetik Algoritma ile çözümlenmiştir. En düşük enerjili yapıların bulunabilmesi için GA çözümlemesinde işlem 2 ila 20 atom aralığı için 200, 20 ila 40 atom aralığı için 400 defa yapılmıştır. Elde edilen yapıların enerjik ve yapısal analizleri yapıldığında, optimize edilen her yapının enerjik olarak durağan ve minimum enerji yayma durumunda olduğu tespit edilmiştir. Optimize edilen yapılar incelendiğinde saf Pt ve Cu yapılarının simetrik ve düzenli, ikili PtCu yapılarının ise 20 atomdan sonra ideal düzenli yapıdan uzaklaştığı görülmüştür. Hem saf hem de ikili Pt-Cu sistemi için, 38 atomdan oluşan yapının tepesi kesik sekiz yüzlü olduğu belirlenmiştir.

Ek olarak, sistemlerin katalitik aktivite ve adsorpsiyon özelliklerini atomistik seviyede incelemek amacıyla ayrı ayrı hidrojen ve moleküler OH adsorpsiyonu incelenmiştir. Adsorpsiyon çalışması Pt_{10}, Cu_{10} ve Pt_3Cu_7 yapıları üzerinde yapılmıştır. H ve OH ile beraber metal sistemlerin yükleri sırasıyla nötr, anyonik ve katyonik durumlarda incelenmiştir. Nötr yük halinin, H ve OH adsorpsiyonu için en uygun olduğu bulunmuştur. Bununla beraber, hem Pt hem de Cu atomunun farklı noktalarına (tepe, köprü ve çukur) adsorpsiyon uygulanmıştır. Saf sistemlerde, hidrojen atomu için adsorpsiyon enerjisinin minimum olduğu durum Pt atomunun tepe bölgesinden iken Cu için köprü pozisyonudur. İkili sistemlerde ise hidrojen atomu Pt atomunun çukur bölgesinden, Cu atomuna göre daha kuvvetle bağlanmaktadır.

ACKNOWLEDGEMENTS

I am grateful for the invaluable guidance I have received throughout my graduate studies from my thesis advisor Prof. Dr. Can Erkey. He have constantly guided me to learn and develop new skills during my years in Koç University. I am thankful for this great opportunity for being a part of excellent community of his group.

I would like to thank to my project coordinator, Dr. Rıza Kızılel for his assistance on Genetic Algorithm and MATLAB as well as for the help and support on this work.

I am very thankful to my thesis committee members Prof. Dr. Ersin Yurtsever and Prof. Dr. Ramazan Yıldırım for their participation to review this document. I also would like to give my sincerest appreciation to Prof. Dr. Ersin Yurtsever for teaching me about Density Functional Theory and Computational Chemistry.

I would like to thank The Scientific Council of Turkey (TUBITAK) for their financial support during my graduate studies.

I am grateful for the support and motivation from my friends during my academic career. Most importantly I thank Yaprak Özbakır for useful discussions, encouragement, priceless support and help throughout the years. Thank you for not only being the exceptional friend but also being the inspiring teacher.

Finally, I am thankful to my parents and brother for their endless support and believe in me in every step of my life. Love you.

TABLE OF CONTENTS

LIST OF TABLES xi
LIST OF FIGURES xii
NOMENCLATURE xiv
1. INTRODUCTION 3
2. LITERATURE REVIEW 6
2.1. Clusters 6
2.2. Structures of Clusters 6
2.3. Applications of Pure and Bimetallic Clusters 7
2.4. Theoretical Background 9
2.4.1. Global Optimization of Clusters 10
2.4.2. Gupta Potential 11
2.4.3. Density Functional Theory 12
2.4.3.1. Thomas-Fermi Model 14
2.4.3.2. The Hohenberg-Kohn Theorems 14
2.4.3.3. Kohn-Sham Theorems 15
2.4.4. Energetic Analysis 15
2.4.4.1. Binding Energy 16
2.4.4.2. Excess Energy 16
2.4.4.3. Second Difference in Energy 16
2.4.5. Structural Analysis 17
2.4.5.1. Average Weighted Bond Length 17
2.4.5.2. Effective Coordination Number 18
2.4.5.3. Second Order Parameter 18
2.4.6. Electronic Analysis 18
2.4.6.1. Detachment Energy (DE) 19
2.4.6.2. Ionization Potential (IP) 19
2.4.7. Adsorption Analysis 19
2.4.8. Global Optimization Methods 20
2.4.8.1. Basin-Hopping (BH) Algorithm 20
2.4.8.2. Genetic Algorithm (GA) 21
3. COMPUTATIONAL METHODOLOGY 24
3.1. GA Method for Structure Determination 24
3.1.1. Determination of parameters for PtCu Clusters 27

3.1.2. MATLAB 28
3.1.3. Supercomputers 28
3.1.4. Avogadro 28
3.2. Atomic Simulations at DFT Level 28
3.2.1. Gaussian 09 29
3.2.2. GaussView 29
3.2.3. Basis Sets 30
3.2.4. Exchange-Correlation (XC) Functional 30
3.2.5. Input File for Gaussian 09 30
4. RESULTS & DISCUSSION 33
4.1. The Effect of the Number of GA Runs on Potential Energies 33
4.2. The Effect of the Number of GA Runs on Cluster Evolution 40
4.3. The Effect of the Number of GA runs on DFT Calculations 58
4.4. Optimized structures of Pt clusters (N=2-40) 60
4.5. Optimized structures of Cu clusters (N=2-40) 62
4.6. Optimized structures of PtCu clusters (N=2-40) 65
4.6.1. Homotop structures of PtCu clusters 67
4.7. Energetic Analysis of Pt, Cu and PtCu Clusters 69
4.7.1. Binding Energy 69
4.7.2. Excess Energy 70
4.7.3. Second Difference in Energy 71
4.8. Structural Analysis of Pt, Cu and PtCu Clusters 73
4.8.1. Average Weighted Bond Length 73
4.8.2. Effective coordination number of Pt, Cu and PtCu clusters 74
4.8.3. Second order parameter 75
4.9. DFT Optimization of PtCu Clusters 77
4.9.1. Energetic Analysis 78
4.9.2. Structural Analysis 78
4.9.3. Electronic Analysis 80
4.10. Adsorption Study at DFT Level 81
4.10.1. Pt Cluster with H atom and OH Molecule 81
4.10.1.1. Adsorption Properties of H and OH on Pt_{10} Cluster in Different Charge States 82
4.10.1.2. Adsorption Properties of H atom on Pt_{10} Cluster on Different Sites 84
4.10.2. Cu Cluster with H atom and OH Molecule 85

4.10.2.1. Adsorption Properties of H and OH on Cu_{10} Cluster in Different Charge States……..... 85
4.10.2.2. Adsorption Properties of H atom on Cu_{10} Cluster on Different Sites..... 87
4.10.3. PtCu Cluster with H Atom and OH Molecule 88
4.10.3.1. Adsorption Properties of H and OH on Pt_3Cu_7 Cluster in Different Charge States……..... 88
4.10.3.2. Adsorption Properties of H atom on Pt_3Cu_7 Cluster on Different Sites ... 90
5. CONCLUSION..... 93
REFERENCES 95
APPENDIX..... 99

LIST OF TABLES

Table 1. The parameters of Pt-Pt and Cu-Cu clusters for Gupta potential [35] 27
Table 2. Calculated potential parameters of Pt-Cu 27
Table 3. The number of times the lowest energy structures (LES) were found and minimum potential energies for pure Pt and Cu and PtCu clusters composed of 2-40 atoms in 100 GA runs 34
Table 4. The number of times the lowest energy structures (LES) were found and minimum potential energies for pure Pt and Cu and PtCu clusters composed of 2-40 atoms in more than 100 GA runs 40
Table 5. Accepted the lowest potential energies (V_{min}/eV) obtained in more than 100 GA runs for pure Pt clusters consisting of up to 40 atoms 60
Table 6. Accepted the lowest potential energies (V_{min}/eV) obtained after more than 100 GA runs for pure Cu clusters consisting of up to 40 atoms 63
Table 7. Accepted the lowest potential energies (V_{min}/eV) obtained in more than 100 GA runs for PtCu clusters consisting of up to 40 atoms 65
Table 8. Potential energy (eV) values of optimized neighboring compositions of PtCu clusters (N=2-40 atoms) 72
Table 9. Adsorption properties of H and OH on Pt_{10} in neutral, anionic and cationic charge states 83
Table 10. The total and adsorption energy of hydrogen on Pt_{10} cluster in top, bridge and hollow site 84
Table 11. Adsorption properties of H and OH on Cu_{10} in neutral, anionic and cationic charge states 87
Table 12. The total and adsorption energy of hydrogen on Cu_{10} cluster in top, bridge and hollow site 88
Table 13. Adsorption properties of H and OH on Pt_3Cu_7 in the neutral, anionic and cationic charge states 90
Table 14. The total and adsorption energy of hydrogen Pt_3Cu_7 cluster from top, bridge and hollow site of Pt and Cu atoms. 91

LIST OF FIGURES

Figure 1. Various structures for different size of clusters (X is the symbolic representation of atom type and subscript represents the number of atoms) 7
Figure 2. Different structures of Pt_{40} cluster 7
Figure 3. The Gupta potential for Pt_2 12
Figure 4. Potential energy surface in the BH-energy minimization. Initially created clusters which are in the same basin of attraction (e.g. A and A') are minimized to the same structure (A_0) while cluster B minimizes to B_0 [70]. 21
Figure 5. Flowchart of GA written in MATLAB language 26
Figure 6. Input file of Pt_{10} cluster created in GaussView for submission to Gaussian 09 32
Figure 7. Percentage of the number of GA runs which gave the lowest potential energy in 100 GA and more than 100 GA runs for Pt and Cu clusters composed of 2-40 atoms .. 37
Figure 8. Percentage of the number of GA runs which gave the lowest potential energy in 100 GA and more than 100 GA runs for PtCu clusters composed of 2-40 atoms 39
Figure 9. Energetic and structural evolution of $Pt_{15}Cu_{15}$ in GA with the number of GA runs ((a) initially created structure, (b) optimized structure at run 134 (local minima), (c) optimized structure at run 377 (global minima)) (Pt atoms are represented in grey and Cu atoms are represented in yellow) 41
Figure 10. The comparison of average processing time for Pt-Cu clusters of 2-40 atoms based on starting point of optimization (red line represent the mean processing time per run when the optimization starts from randomly initialization, black line represents the mean processing time per run when the optimization starts from the previously optimized cluster size) 58
Figure 11. Energetic, structural and processing time properties of the lowest energy structures obtained in 1 GA run, in 100 GA runs and in 400 GA runs on DFT calculations 59
Figure 12. The lowest energy structures of Pt clusters consisting of 2–40 atoms 62
Figure 13. The lowest energy structures of Cu clusters consisting of of 2-40 atoms 64
Figure 14. The lowest energy structures of PtCu clusters with 2-40 atoms 67
Figure 15. Potential energies and morphologies of homotopic structures for PtCu clusters composed of 12, 20, 26, 28 and 34 atoms 68
Figure 16. Two homotops for the $Pt_{10}Cu_{10}$ cluster is in the left and for $Pt_{14}Cu_{14}$ is in the right. First column in both side showed the homotops in 3D while second column in 2D arrangements. 69
Figure 17. GA binding energies for pure Pt, Cu and Pt-Cu clusters with N=2-40 atoms 70
Figure 18. GA excess energies of local and global minima for PtCu clusters with N=2-40 atoms 71
Figure 19. Second difference in energy for PtCu clusters (N=2-40 atoms) at the Gupta potential level 73
Figure 20. Calculated average bond lengths for pure Pt, Cu and Pt-Cu clusters consisting of 2-40 atoms 74
Figure 21. ECN values of Pt, Cu and PtCu clusters (N=2-40 atoms) 75
Figure 22. Second order parameter (σ) for PtCu clusters consisting of 2-40 atoms 76

Figure 23. Optimized structures and total energies of each composition of 10 atoms of PtCu clusters at DFT level 77
Figure 24. DFT excess energies as a function of Pt atoms in the Pt_nCu_{10-n} 78
Figure 25. Calculated average bond lengths as a function of Pt atoms in the Pt_nCu_{10-n} cluster 79
Figure 26. ECN as a function of Pt atoms in the Pt_nCu_{10-n} cluster 80
Figure 27. Detachment energy and ionization potential as a function of Pt atoms in the Pt_nCu_{10-n} 81
Figure 28. The lowest energy structures and total energies of adsorbed H and OH on Pt_{10} cluster in neutral, anionic and cationic charge states (Pt is represented by grey and hydrogen is white while oxygen is represented by red) 82
Figure 29. The lowest energy structures for the hydrogen adsorption on Pt_{10} cluster on different sites 84
Figure 30. The lowest energy structures and total energies of adsorbed H and OH on Cu_{10} cluster in neutral, anionic and cationic charge states (Cu is represented by yellow and hydrogen is by white while oxygen is represented by red) 86
Figure 31. The lowest energy structures for the hydrogen adsorption on Cu_{10} cluster on different sites 87
Figure 32. The lowest energy structures and total energies of adsorbed H and OH on Pt_3Cu_7 cluster in neutral, anionic and cationic charge states 89
Figure 33. The lowest energy structures for the hydrogen adsorption on Cu_{10} cluster on different sites 91

NOMENCLATURE

r_0	*Equilibrium first neighbor distance in fcc solid*
r_{ij}	*Equilibrium bond distance between atom i and j*
V_{clus}	*Cluster potential energy in eV*
N	*Total number of atoms*
E_{exc}^{Gupta}	*Excess energy calculated at Gupta level in eV*
E_b^{Gupta}	*Binding energy calculated at Gupta level in eV*
$\Delta_2 E$	*Second difference in energy in eV*
d_{av}^i	*Averaged weighted bond lengths in A^o*
ECN	*Effective coordination number*
d_{ij}	*Distance between atom i and j in A^o*
σ	*Second order parameter*
DFT	*Density Functional Theory*
GA	*Genetic Algorithm*
EAM	*Embedded Atom Model*
MD	*Molecular Dynamics*
MC	*Monte Carlo*
SMTAB	*Second moment to tight binding*
a.u.	*Atomic unit (in Hartree)*
DE	*Detachment energy*
IP	*Ionization Potential*
BH	*Basin Hopping*
LDA	*Local density approximation*
GGA	*Generalized gradient approximation*

1. INTRODUCTION

Supported alloys of Pt nanoparticles with relatively cheap transition metals (TM) such as Fe [2, 3], Co [4-6], Ni [7-9], Cu [10-13], and Zn [14, 15] have attracted great interest as alternatives to supported pure Pt catalysts. Such nanoparticles may also show improved electro-catalytic activity for the oxygen reduction reaction (ORR) [16, 17] which is crucial for widespread use of polymer electrolyte membrane fuel cells [18, 19]. Previous experimental and theoretical studies showed that the particle size, morphology (i.e. core-shell, segregated, disordered alloy) [20] and composition of these bimetallic nanoparticles are important factors which effect the rate of the ORR. Therefore, the determination of the most stable structure of such nanoparticles is an essential step in understanding their catalytic properties.

Prediction of structures of bimetallic nanoparticles have been widely studied by a wide variety of theoretical approaches. However, finding energetically favourable structures is computationally intensive, in particular due to the exponential increase of the number of local minima configurations with the increasing number of atoms [21]. For example, in a PtCu nanoparticle with a diameter of 4 nm, there are *N=2212* atoms. The total number of geometric isomers for such a nanoparticle can be calculated using $\frac{N!}{N_{Pt}!\,N_{Cu}!}$ which gives almost an infinite number of possible isomers. Moreover, the number of homotops, [22] which are defined as isomers with the same geometry and composition but with different atomic arrangements of two types of atoms, for such a nanoparticle is $\mathbf{2}^{\mathbf{2212}}$. Therefore, such a large number of possibilities of geometrical isomers and homotops have made searching global minima computationally very time consuming.

Metal clusters have been studied to model energetically most stable morphologies of heterogeneous catalysts and to reduce computational cost. Clusters are composed of fewer atoms than a nanoparticle and their size is usually less than 2 nm [23]. Since their properties evolve with changes in size, they can be controlled to fabricate material with desirable properties on the nano-scale. Therefore, the effects of composition, size and atomic ordering [24] on physical and chemical properties [25] of nanoparticles can be understood by carrying out simulations with clusters. To this end, information on the chemical reactivity or catalytic activity of nanoparticles have been obtained by approximating it as a cluster [20].

One of the most accurate global optimization [26] approach for finding the atomic arrangements of small size of clusters at their ground state which corresponds to their lowest potential energy, i.e. Global Minimum (GM) [27] is Density Functional Theory (DFT) [28-30]. Theoretical predictions by DFT strongly match with experimental results and give important information on geometric, electronic and spectroscopic properties of the systems being studied. Although DFT has high accuracy up to a few hundred atoms, calculations become very time consuming and computationally expensive as the number of atoms in the cluster become larger [31].

Alternatively, evolutionary algorithms combined with several semi-empirical potentials such as Lennard-Jones [32], Sutton-Chen [33], Born-Mayer [34] and Gupta [35] which describe rather realistically the interatomic interactions amongst cluster atoms, have been commonly used in studies on clusters for various sizes and compositions. Gupta semi-empirical potential [36] which was derived from Gupta's expression for cohesive energy of bulk material is based on the second moment approximation of a tight-binding Hamiltonian (SMATB model) [35, 37]. Gupta potential has been iteratively solved coupled with Genetic Algorithm (GA) [38-40] which is a powerful and efficient searching algorithm for optimization problems.

For structure determination of clusters, creating initial clusters is an important factor for global optimization at high level of theory such as DFT. Feeding randomly arranged structures to DFT increases processing time and prevents the finding of the lowest energy structure of the cluster. It is well known that initial clusters which resembles closely the lowest energy structure were generated using semi-empirical potentials with evolutionary algorithms. However, it can be pointed out that current understanding on cluster optimization using GA and DFT is still unclear and several key aspects remain unexamined. For example, the optimum GA runs that have to be done to reach minimum energy structures in the case of both monometallic and bimetallic clusters are not known. Secondly, structural and energetic differences in the morphologies obtained in more than 100 GA runs have not been studied. Moreover, site preference of H atom and OH molecule and the effect of adsorbed molecule on energetic changes of clusters at atomistic level is far from satisfactory.

In this study, a brief review of literature studies on clusters and global optimization is provided in Chapter 2. Chapter 3 outlines the computational methods used including 100 GA runs, the effect of the extended number of GA runs up to 400 on structure determination at Gupta and at the DFT level. Chapter 4 covers the results for optimized structures of Pt, Cu and PtCu clusters consisting of up to 40 atoms at Gupta level as well as DFT calculation of each composition of 10 atoms of PtCu clusters. Chapter 4 also includes the results on adsorption of one hydrogen atom and OH molecule on Pt, Cu and PtCu clusters from different sites such as top, bridge, hollow and gives adsorption properties in the different charge states. Chapter 5 provides a summary and future directions.

2. LITERATURE REVIEW

2.1. Clusters

Experimental and theoretical studies on clusters have attracted great interest in both basic science and applications since the physical and chemical properties of clusters are different from their corresponding bulk counterparts. Their physical and chemical properties can be controlled by changes in their size, structure and composition [27].

Studies on clusters were started in developing experimental techniques and characterization methods. E.W Becker was performed the first experiment on clusters using mass spectrometer ion source in 1956 [41]. Starting from 1980s, laser vaporization techniques led to the synthesis of most of the elements of periodic table as in their cluster forms. However, experimental techniques still unable to determine structures of clusters. By the 1990s, theoretical approaches have become crucial on structure determination. The developments in global optimization methods using evolutionary algorithms and first principle calculations with the help of enhanced supercomputer power made it possible to determine the structures of clusters consisting of up to a few hundred atoms [27].

In both physics and chemistry, clusters are defined as aggregates of countable number of atoms [24]. As the cluster size increases, the surface to bulk ratio gets smaller. When clusters are small and their surface-to-volume ratio is high, they have more atoms lie on the surface compared to their bulk-phase [20]. Therefore, surface structure of clusters is very important factor which determines their physical and chemical properties.

2.2. Structures of Clusters

The geometric structures of pure and bimetallic clusters dominate their corresponding physical and chemical properties. Several possible structures which exhibit

different properties can be seen in cluster regime. Various structures for different cluster size are shown in Figure 1.

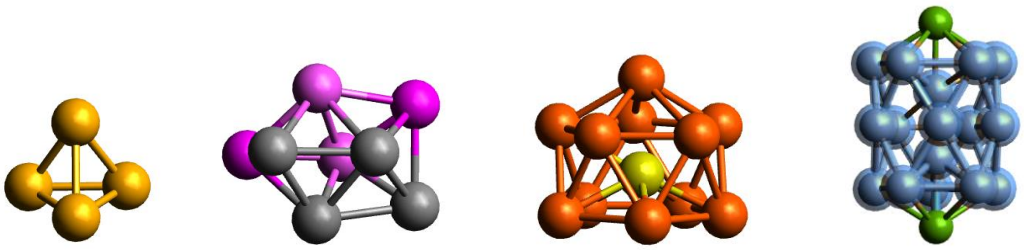

X_4 X_6 X_{12} X_{18}

Figure 1. Various structures for different size of clusters (X is the symbolic representation of atom type and subscript represents the number of atoms)

One example is the different isomers of Pt_{40} cluster can be seen in Figure 2. Pt_{40} atoms have 3 different structures as layer-by layer, distorted icosahedron and hexagonal antiprism. Calculations on these various structures showed that the layer-by-layer structure of Pt_{40} which is seen in Figure 2(a) has energetically more stable ordering compared to its corresponding distorted isomers.

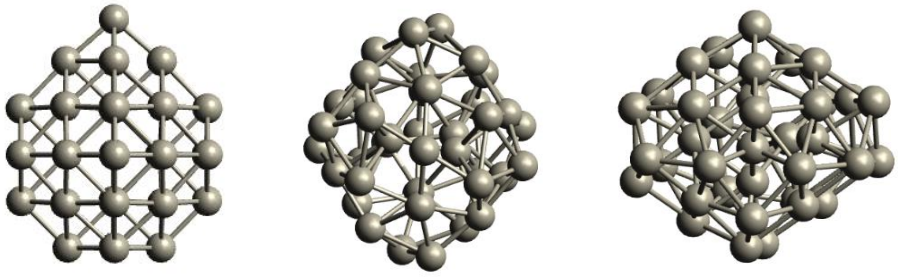

(a) Pt_{40}-layered (b) Pt_{40}- icosahedral (c) Pt_{40}-hexagonal antiprism

Figure 2. Different structures of Pt_{40} cluster

2.3. Applications of Pure and Bimetallic Clusters

Generally, noble metal clusters are shown significant improvements on developing new materials for clean and low-cost energy production. Pt clusters are extensively studied because of their importance in catalysis. It is well known that Pt

catalyst shows impressive electrocatalytic behavior over oxygen reduction reaction (ORR) in fuel cells. In 2013, Markus *et. al.* [42] investigated how small size of Pt cluster compared with Pt nanoparticle behave as superior catalyst. They showed that size selected Pt nanoclusters (between 0.6 nm and 2.3 nm diameter) can reach extraordinarily high ORR activity under high Pt coverage on a glassy carbon substrate and arranged very close distance between small particles [42].

Cu is considerable interest in synthesizing nanoalloys since its relatively cheaper cost and high abundancy compared to Pt. It helps reducing the catalyst cost while increasing the catalytic properties.

Bimetallic clusters are mainly studied to reduce catalyst cost and improve power conversion efficiency. Recent experimental studies have focused on the Pt-based nanoparticles to effectively improve both the kinetics of the catalytic reactions and utilization of Pt while reducing the amount of Pt because of its high cost and limited reserve. Starting from 1970s, the combination of Pt-Cu has been used as a catalyst for many reactions such as CO oxidation [43], NO_x reduction [44] and hydrocarbon reforming [45]. By 2000, Pt-Cu nanoparticles has studied as an alternative catalyst compared to pure Pt especially in the fuel cell. In 2008, Mani *et. al*., showed that dealloyed catalyst consisting with Cu-rich core surrounded by multilayer Pt-rich shell had more than factor of 4 mass activity compared to Pt electrocatalysts [46]. In 2010, Dutta *et. al*., synthesized Pt-Cu nanoparticles and characterized the alloy structure using high-angle annular dark-field scanning transmission electron microscopy (HAADF STEM) and X-ray absorption spectroscopy (XAS) [47]. Both STEM and XAS showed that good ORR activity was reached during Pt-shell on a Cu-rich core formation. Although Pt-Cu catalysts have been widely studied, experimental techniques do not provide information on structural formation in the atomistic level. Therefore, theoretical investigations are needed to obtain better understanding of the structural information which have a direct

effect on catalytic activity. Clusters have become important and attracted great interest since they fill the gap between atomic level and nanometer scale. To get deep understanding on formation at atomic level and guide future experiments, structure determination have been studied with clusters theoretically.

In 1993, Cleri and Rosato investigated the Gupta potential parameters of Pt and Cu clusters experimentally [35] . Studies continued with the structure determination of bimetallic clusters using Genetic Algorithm coupled with Gupta potential. Johnston *et al.*, showed that Pt-Pd clusters consisting of up to 20 atoms and each composition of 34 atoms. The lowest energy structures which obtained 100 GA run were presented as global minima. In 2002, Darby *et al*., presented the global minima structures of pure Cu up to 56 atoms obtained within GA coupled with Gupta potential [48] . Further, re-optimization at the DFT level was studied to find physical and chemical properties of the system being studied. In 2015, Chaves *et al*. showed that high and low energy isomers of PtCu clusters consisting of up to 14 atoms [21] . Further, they investigated energetic, structural, magnetic and electronic properties of each composition of 55 atoms of PtCu clusters at the DFT level [49] . In all of these studies at high level of theory, initial clusters for DFT calculations were taken from GA or Monte Carlo simulations. Although, it is well known that DFT calculations strongly depend on the initial structures, studies do not show the effect of initialization procedure on the lowest energy structures in both Gupta and DFT level. In this thesis, we analyzed the optimum number of GA runs has to be done to reach the lowest energy structures of Pt, Cu and PtCu clusters. Also, the effect of the number of GA runs on energetic and structural stability of clusters at the DFT level.

2.4. Theoretical Background

The idea of structure determination started with Born-Oppenheimer approximation [50]. It is indicated that the lowest energy structure of the system being

studied is calculated as a function of atomic positions (i.e. coordinates). Potential energy surface (PES) is a function of atomic coordinates of all atoms in the cluster and is represented by *E(r)* [51]. The searching procedure for the lowest energy configuration on the PES is known as global optimization. The structure which is obtained with the lowest potential energy at ground state is known as global minimum (GM). Details of global optimization of clusters and global optimization methods are explained below.

2.4.1. Global Optimization of Clusters

Global minimum morphologies of clusters can be found using several global optimization approaches. One of the most accurate global optimization approach for small size of cluster structures is DFT. For a large system containing a few tens of atoms, it is very difficult to obtain with the most stable structures on DFT environment. To overcome the complexity of DFT calculations, simpler models which define interatomic interactions within cluster regime are developed. Atomistic second-moment approximation to the tight-binding model (SMATB) is used as more appropriate solution method for structure optimization. The atomistic models allows to build possible structures in a very short time with good qualitative and quantitative results up to a few hundred atoms. They are also less computationally intensive (computationally low-cost) compared to DFT.

In the atomistic model, the energy of the cluster, which is denoted by *E*, can be calculated with the sum of repulsive and attractive forces acting on the each atom in cluster. In the atomistic model, semi-empirical potential energy models such as Lennard-Jones [32], Sutton-Chen [33], Born-Mayer [34] and Gupta [35] are used to define atomic interactions. In our study, Gupta-type semi-empirical potential energy is used as an energy model (see the explanation below).

2.4.2. Gupta Potential

Semi-empirical Gupta-type many body potential is used to define interatomic interactions within cluster regime. Gupta potential [35, 36] was derived from Gupta's expression for cohesive energy of bulk material and is based on SMATB interaction potential [37, 52, 53].

The Gupta potential is written in terms of Born-Mayer type repulsive part and attractive many body term (V^m) and is expressed as follows [48];

$$V_{clus} = \sum_i^N [V^r(i) - V^m(i)] \tag{2.3}$$

where V^r and V^m are defined as;

$$V^r(i) = \sum_j^N A \exp\left(-p\left(\frac{r_{ij}}{r_0} - 1\right)\right) \tag{2.4}$$

and

$$V^m(i) = \left[\sum_j^N \zeta^2 \exp\left(-2q\left(\frac{r_{ij}}{r_0} - 1\right)\right)\right]^{1/2} \tag{2.5}$$

where r_{ij} represents the distance between ith and jth atoms in the cluster, r_0 is the nearest neighbor distance of crystal at 0 K. A, p, q and ζ are the empirical parameters fitted to experimental values such as cohesive energy, lattice parameters and independent elastic constants for the crystal structure at 0 K [48]. A typical Gupta potential graph for two platinum (Pt) atoms is shown in Figure 3.

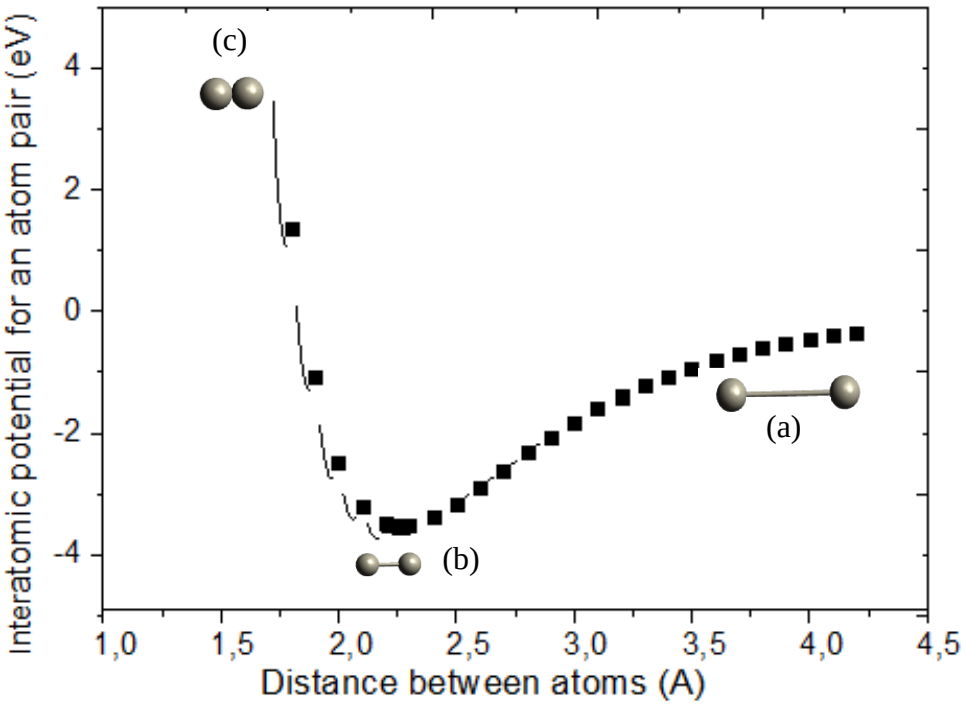

Figure 3. The Gupta potential for Pt_2

Potential energy is negative when separation distance between two atoms are long. As the bond length increases to infinity, potential energy approaches zero. This indicates that attractive force acting on the pair of atoms or molecules when the distance is greater than equilibrium. (see in Figure 3a). Distance between two atoms continues to decrease until the particles reach an equilibrium. At this point, the pair of particles is in the most stable position, specified by the distance at which the minimum potential energy is found. (see in Figure 3b). As the bond distance between two atoms decreases below equilibrium distance, they start to repel each other and their potential energy becomes increasingly positive which indicates a repulsive force (see in Figure 3c).

2.4.3. Density Functional Theory

The structural and spectroscopic properties of the system is quantum mechanically determined by solving the Schrödinger equation. The Schrödinger equation determines how the state which is known as the wave function (ψ) of the particle evolves through

electron interactions. Time-independent Schrödinger equation is expressed as follows [54];

$$\hat{H}\psi = E\psi \tag{2.6}$$

where $\hat{H}$ is the Hamiltonian operator, ψ is the wavefunction and E is the total energy. Once the ψ is known, any properties of the system can be calculated.

Schrödinger equation can only be solved for H_2 molecule. For many body systems which includes more electrons, the equation needs more simplifications with further approximations. Born–Oppenheimer approximation is used which states that the nuclei and electrons are separated individual entities. Since the mass of nuclei 1837 times higher than the electrons, the nuclei are assumed as stationary while electrons move around the nuclei. Therefore, the kinetic energy of nuclei is neglected and the potential energy of the nuclei-nuclei is taken as constant. Within these approximations, the Hamiltonian is expressed as;

$$\hat{H} = \hat{T_e} + \widehat{V_{ee}} + \widehat{V_{ext}} \tag{2.7}$$

where $\hat{T_e}$ is the kinetic energy of electrons, $\widehat{V_{ee}}$ is the potential energy due to interaction between electron-electron and $\widehat{V_{ext}}$ is the attractive potential energy between nuclei and electron (i.e. external potential).

As seen in Equation 2.7, $\widehat{V_{ee}}$ is the term responsible for Coulombic repulsion of two electrons that contains too many degree of freedom. This term includes all the information needed for electronic structure. Still the major challenge on structure determination is calculation of $\widehat{V_{ee}}$ term for systems which contain lots of electrons. Hence, additional approximations are needed to solve Eq. 2.7.

Density Functional Theory (DFT) is probably the most accurate ab-initio method (i.e. first principles) in computational chemistry especially for small sizes. It can properly built electronic properties of the system and determine the structural properties. The

theory of DFT is first introduced by Thomas-Fermi model in 1927 [55] and then improved with the equations provided by Hohenberg-Kohn in 1964 [56] and followed by Kohn-Sham in 1965 [57]. Developments through DFT approach are summarized below.

2.4.3.1. Thomas-Fermi Model

The Thomas and Fermi model is known as the first DFT approach presented in 1927. The basic idea of the Thomas and Fermi model states that the total energy of the system could be expressed as a functional, which is a function of electron density [58]. This theory has good predictive capability but it does not accurately present the orbital structures of electrons. And thus, it is considered as a crude model for many body systems. For larger systems which contains lots of electrons, more accurate models which are Hohenberg-Kohn and Kohn-Sham equations were developed.

2.4.3.2. The Hohenberg-Kohn Theorems

Hohenberg and Kohn theorems are based on minimization of square of the wavefunction. It stated two important theorems which are explained below:

Theorem I: The total energy of a system at ground state is a unique functional of the ground state electron density $(n(r))$ [56, 59]. Electron density directly responsible for the external potential, $\widehat{V_{ext}}$. Hence, all the physical and chemical properties of the system can be found, if the electron density (denoted by$(n(r))$ is known.

Theorem II: The second theorem is known as the variational principle [60]. This theorem states that the total energy can be found by minimizing the energy functional with respect to the electron density, $n(r)$.

According to these findings, the total energy could be written as;

$$E[\rho] = T[\rho] + U[\rho] + E_{XC}[\rho] \tag{2.8}$$

where T is the kinetic energy of the non-interacting particles, U is the electrostatic energy due to Coulombic interactions and E_{XC} is the exchange and correlation which includes many-body interactions to total energy calculations.

Although the Hohenberg-Kohn theorems could be improved to by considering the number of electron in the system, it does not provide the ground state energy. Only an electron interaction with mean electron field is considered and thus electron-electron interaction missed. This part was developed by Kohn and Sham in 1965.

2.4.3.3. Kohn-Sham Theorems

In 1965, Kohn and Sham successfully proved that the ground state of the system can be calculated by considering the many body system as one electron system [57]. Energy minimization cycle (see in Eq. 2.8) determines the electron density and E_{XC} part. This procedure can be led by Kohn and Sham assumptions.

After several years with these developments on many body systems, DFT has become a powerful method in computational chemistry. DFT calculations can work effectively for global optimization of small size of clusters. Although DFT is more accurate model to describe the system, it is a computationally expensive and time consuming process. Nowadays supercomputers with a high capacity and speed are required for larger clusters. Even for a small size of clusters, pure DFT calculations could take days or weeks. Therefore, semi-empirical potentials like Gupta which describes interatomic interactions in many body systems can be used as good approximation for global optimization problems of larger size of clusters.

2.4.4. Energetic Analysis

Energetic stabilities of clusters are needed to be calculated to check whether the optimized structures are dynamically stable or not. Three important criteria, namely (a)

binding energy, (b) excess energy and (c) second difference in energy are calculated as follows.

2.4.4.1. Binding Energy

The first energetic quantity is the *average binding energy* $\left(E_b^{Gupta}\right)$. This quantity can be calculated per atom of a cluster as follows [48];

$$E_b^{Gupta} = -\frac{V_{clus}}{N} \tag{2.9}$$

where V_{clus} is the total potential energy of a cluster (monometallic or bimetallic) and N is the total number of atoms. The positive average binding energy indicates that cluster has energetically stable atomic arrangement.

2.4.4.2. Excess Energy

The excess energy is another energetic quantity which indicates the energy associated with the existence of second metal. Excess energy is defined for Pt_mCu_n cluster as follows [61, 62];

$$E_{exc}^{Gupta}(Pt_mCu_n) = E(Pt_mCu_n) - (N-m)\frac{E(Cu_N)}{N} - (N-n)\frac{E(Pt_N)}{N} \tag{2.10}$$

where $E(Pt_mCu_m)$, $E(Cu_N)$ and $E(Pt_N)$ are the potential energies of bimetallic and monometallic clusters of $N = m + n$ atoms calculated at Gupta level. The negative excess energy indicates that bimetallic clusters are energetically favorable compared to their pure counterparts.

2.4.4.3. Second Difference in Energy

Another important criteria to determine energetic stability of clusters is the *second difference in energy* $(\Delta_2 E(Pt_mCu_n))$ with respect to the neighboring compositions and is given by [63, 64];

$$\Delta_2 E(Pt_m Cu_n) = E(Pt_{m+1} Cu_{n-1}) + E(Pt_{m-1} Cu_{n+1}) - 2E(Pt_m Cu_n) \qquad (2.11)$$

If the binding energy of $Pt_m Cu_n$ is larger than that of its two neighboring compositions, $\Delta_2 E(Pt_m Cu_n)$ needs to be positive for the lowest energy clusters.

2.4.5. Structural Analysis

Several methods [65] such as Common Neighbor Analysis, Bond Angle Analysis, Bond Order, Effective Coordination Number and Neighbor Distance Analysis have been introduced with the aim to get a deeper understanding of how structural properties of the clusters evolve when their atomic coordination become symmetric or distorted. Here, effective coordination number concept is applied to analyze structural formation of clusters. Averaged weighted bond length and effective coordination number of clusters are calculated by creating a special algorithm in MATLAB® which can be seen in the Appendix.

2.4.5.1. Average Weighted Bond Length

Effective coordination number concept is based on the effective coordination number (ECN_i) and the average weighted bond lengths (d_{av}^i) [66-68]. d_{av}^i can be calculated for each atom i [67],

$$d_{av}^i = \frac{\sum_j d_{ij} exp\left[1-\left(\frac{d_{ij}}{d_{av}^i}\right)^6\right]}{\sum_j exp\left[1-\left(\frac{d_{ij}}{d_{av}^i}\right)^6\right]} \qquad (2.12)$$

where d_{ij} represents the distance between atom i and the surrounding atom j. The shortest bond length for atom i is assigned as an initial value and d_{av}^i is determined iteratively.

2.4.5.2. Effective Coordination Number

ECN_i is obtained for each ij pair by the following equation by using calculated d_{av}^{i} [67],

$$ECN_i = \sum_j exp\left[1 - \left(\frac{d_{ij}}{d_{av}^{i}}\right)^6\right] \quad (2.13)$$

Each atom in the cluster has a bond length and an effective coordination number. The average values for both bond length and effective coordination number are calculated by summing all ECN_i and d_{av}^{i} values of each atom and dividing it by the total number of atoms (N) in the cluster.

2.4.5.3. Second Order Parameter

Even though ECN is a useful concept to understand the relationship between structure stability and size, it gives no information on the number of homo- and hetero bonds in bimetallic clusters. In order to investigate the distribution of Pt and Cu atoms in bimetallic clusters, chemical order parameter (σ) is calculated using [69]:

$$\sigma = \frac{N^{Pt-Pt} + N^{Cu-Cu} - N^{Pt-Cu}}{N^{Pt-Pt} + N^{Cu-Cu} + N^{Pt-Cu}} \quad (2.14)$$

where N is the total number of bonds between Pt-Pt, Cu-Cu and Pt-Cu. According to the previous studies, σ is positive when segregation takes place, is close to zero when disordered mixing occurs and negative when homogeneous mixing occurs [70].

2.4.6. Electronic Analysis

In order to investigate electronic properties which gives an information on reactivity of clusters, detachment energy (DE) and ionization potential (IP) are calculated.

2.4.6.1. Detachment Energy (DE)

Detachment energy is the energy needed to remove an electron from a negative ion in its ground state with freezing the internuclear distance. It is also defined as the negative of the affinity. The DE of PtCu clusters are calculated using the following equation [21];

$$DE = E_{tot}(Pt_mCu_n)^0 - E_{tot}(Pt_mCu_n)^- \quad (2.15)$$

where $E_{tot}(Pt_mCu_n)^0$ and $E_{tot}(Pt_mCu_n)^-$ are the total energy of the neutral and anionic state of PtCu clusters calculated by DFT.

2.4.6.2. Ionization Potential (IP)

Ionization potential is the energy needed to remove an electron from a neutral atom to form cation in its ground state without changing the internuclear distance. The IP of PtCu clusters are calculated using the following equation [21],

$$IP = E_{tot}(Pt_mCu_n)^+ - E_{tot}(Pt_mCu_n)^0 \quad (2.16)$$

where $E_{tot}(Pt_mCu_n)^+$ and $E_{tot}(Pt_mCu_n)^0$ are the total energy of the cationic and neutral state of PtCu clusters calculated by DFT.

2.4.7. Adsorption Analysis

Bimetallic clusters have enhanced reactivity for many reactions catalyzed by heterogeneous catalysts compared to their pure counterparts. To get deep understanding on their activity properties, adsorption of one hydrogen atom and OH molecule on pure Pt, Cu and PtCu clusters were studied in this thesis. Adsorption strength between adsorbate and metallic atom is found via the adsorption energy calculation. Adsorption energy is calculated using the following equation,

$$E_{ads} = (E_{ads+cluster})^{\pm/0} - E_{cluster}{}^{\pm/0} - E_{adsorbate} \quad (2.17)$$

where$(E_{ads+cluster})^{\pm/0}$ is the total energy for the system composed of adsorbed species on cluster in the different charge states, namely anionic, cationic and neutral, $E_{cluster}$ is the total energy of pure cluster without adsorbate in the different charge states and $E_{adsorbate}$ is the total energy of adsorbate which is hydrogen and OH energy in our case.

2.4.8. Global Optimization Methods

Finding the lowest energy structures of metal clusters is difficult task since the possible isomers increases exponentially when cluster size become larger. Basin Hopping (BH) and Genetic Algorithm (GA) are two optimization tools for structure determination. In this thesis, GA method was used for structure determination of clusters.

2.4.8.1. Basin-Hopping (BH) Algorithm

Monte Carlo based BH algorithm is an energy minimization algorithm for global optimization. BH algorithm starts to generate new clusters and iteratively minimizing the potential energy of created each cluster. Each energetically minimized cluster are taken as local minima. Finding global minima in a large number of possible local minima highly depends on the number of iteration. Waley and Doye proved that combination with BH and Lennard-Jones potential would accurately find the lowest energy structures up to a few hundred atoms [71]. They pointed out that searching the lowest energy structure is an iterative process where each iteration corresponds to a local minimum on the PES. This process is shown in Figure 4.

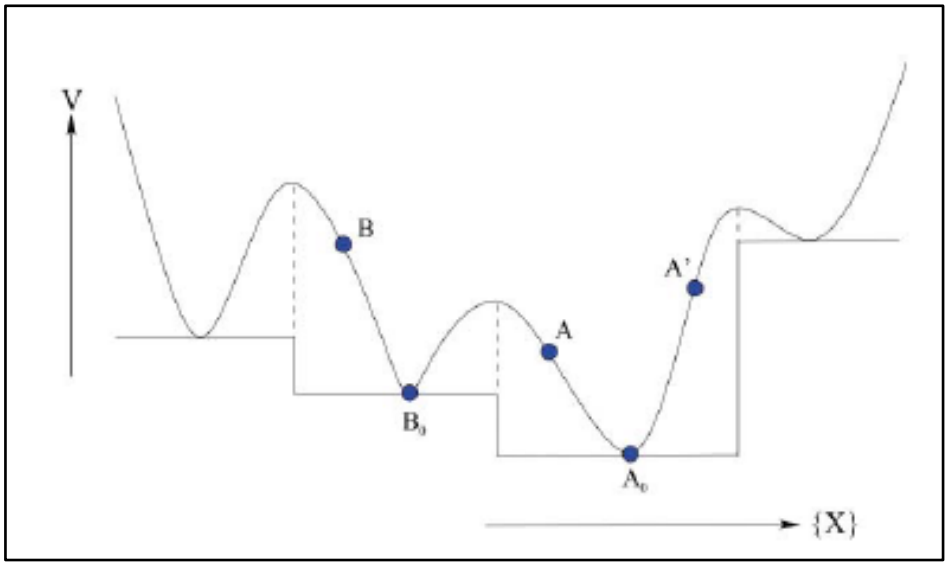

Figure 4. Potential energy surface in the BH-energy minimization. Initially created clusters which are in the same basin of attraction (e.g. A and A') are minimized to the same structure (A_0) while cluster B minimizes to B_0 [72].

Searching efficiency of BH algorithm strongly depends on the type of moves to generate new configurations. Some important and useful moves are: Shake move, Brownian move, Shell move and Exchange move [73].

2.4.8.2. Genetic Algorithm (GA)

The GA is a method to find the minimum energy structures of atomic clusters. Compared to BH algorithm, GA is faster and provide larger solutions for possible structures. Studies on global optimization of clusters using GA method was first carried out by Hartke [74]. The main idea behind GA is natural evolution. GA produces random generations where the population is composed of candidate solutions. Briefly, a specific size of population which is composed of randomly generated clusters are locally minimized with respect to the defined potential representation which is Gupta potential in this study. Each cluster has its own fitness function. Fitness function indicates the energetic quality of clusters. If the fitness value is high, it means the potential energy of cluster is low which reliable case is. Next, best two clusters are selected as parents for

reproduction cycle. To increase the diversity of population, crossover and mutation operators are applied. These two operators allows to reach structures with a lower energy. This whole cycle is repeated where the convergence criteria is reached. Detailed information on GA methodology is explained in Chapter 3.

3. COMPUTATIONAL METHODOLOGY

3.1. GA Method for Structure Determination

The GA method coupled with Gupta many body potential is used to determine the lowest energy structures of pure Pt, Cu and PtCu clusters consisting of up to 40 atoms. GA code is written in MATLAB® language. GA code and its operators can be seen in the Appendix. Here, the methodology of GA is explained as follows:

1. Optimization was started with generating a fixed size population of N random geometries. In this study, 10 random geometries were generated as initial configurations. These randomly created initial geometries differed from each other with respect to the Cartesian coordinates of each atom in the cluster.
2. After initial populations were created, each cluster were relaxed into the nearest local minima by minimizing Gupta potential energy by varying the Cartesian coordinate of each atom.
3. After the initial structures were locally minimized, fitness values of each cluster were calculated. The highest fitness value indicates that the cluster has the lowest potential energy (i.e. more negative potential energy) while the lowest fitness function corresponds to the cluster which has the highest potential energy (i.e. energetically unfavorable). The fitness function was given by hyperbolic tangent of dynamic scaling factor which indicates the energetic quality of cluster to be selected for further generation.
4. In selection part, roulette wheel method was applied. In this type of selection, clusters which have low potential energy (high fitness) were kept for selection as parents. Characteristic properties of selected parents were passed to the next generation by applying crossover operator.

5. The single cut method was applied as crossover operator to two parent clusters. Both parent clusters were cut horizontally into two parts. The top half of the parent 1 and the bottom half of the parent 2 were glued them together to produce a new offspring.
6. The number of offspring was chosen as 80% of the population size. Energetic minimization continued through each offspring formation.
7. In order to prevent offspring set in local minima, mutation operation was applied. Cluster replacement for pure clusters while atom permutation for bimetallic clusters were chosen as mutation operator with a rate of 0.1.
8. After mutation, each "mutant" was minimized and ordered according to their fitness values using procedure as described in Figure 1.
9. This process was repeated until the optimization criteria which is the potential energy difference between the best individual of the final population and the best individual of all was 10^{-5} eV/atom was reached.
10. Individuals with the lowest energy in the final generation were stored.

The schematic representation of algorithm between steps of 1-10 is shown in Figure 4. This procedure is the definition of only 1 GA run. In this study, for the first time the whole procedure given in Figure 5 was extended up to 400 GA runs starting from randomly generated populations of 10).

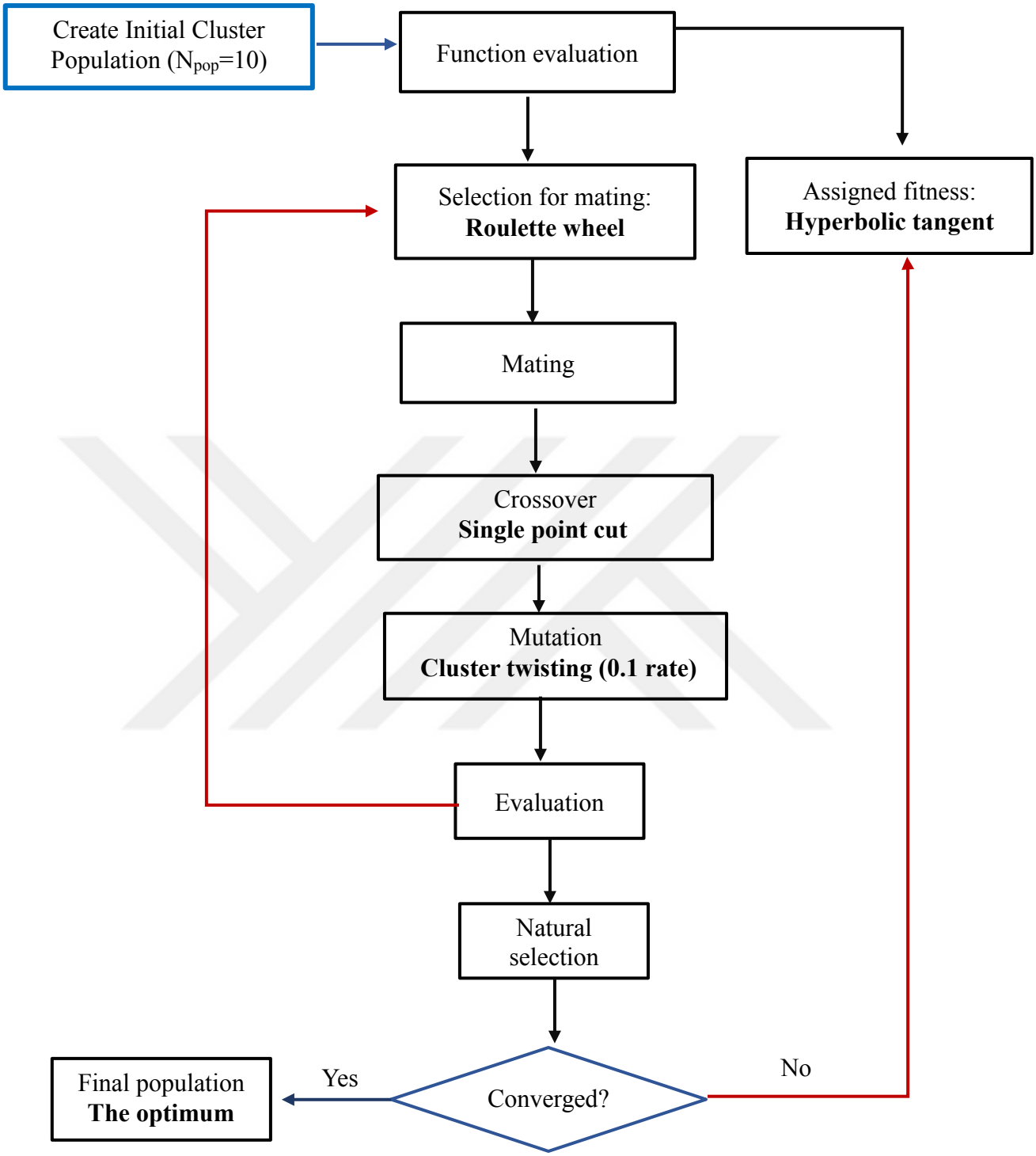

Figure 5. Flowchart of GA written in MATLAB language

3.1.1. Determination of Parameters for PtCu Clusters

The Gupta potential parameters which describe Pt-Pt and Cu-Cu interactions are listed in Table 1.

Table 1. The parameters of Pt-Pt and Cu-Cu clusters for Gupta potential [35]

Parameters	Pt-Pt	Cu-Cu
$\boldsymbol{A}$ **/eV**	0.2975	0.0855
$\boldsymbol{\zeta}$**/eV**	2.6950	1.2240
$\boldsymbol{r_0}$**/A°**	2.7747	2.5560
$\boldsymbol{p}$	10.612	10.960
$\boldsymbol{q}$	4.004	2.2780

In 1993, Cleri and Rosato [35] found that the parameters of fcc-based clusters can be calculated by taking their weighted averages as follows;

$$P(Pt-Cu) = zP(Pt-Pt) + (1-z)P(Cu-Cu) \tag{3.1}$$

where P indicates Gupta potential parameter and z is the atomic composition factor. In this study, z was taken as 0.5 since atomic composition of 1:1 of PtCu bimetallic clusters were studied. Calculated potential parameters of PtCu clusters in this study are presented in Table 2.

Table 2. Calculated potential parameters of Pt-Cu

Parameters	Pt-Cu (z=0.5)
$\boldsymbol{A}$ **/eV**	0.1915
$\boldsymbol{\zeta}$**/eV**	1.9595
$\boldsymbol{r_0}$**/A°**	2.6653
$\boldsymbol{p}$	10.7860
$\boldsymbol{q}$	3.1410

3.1.2. MATLAB

The GA code coupled with Gupta many body potential is written in MATLAB® which is a well suited computing language for optimization problems. It is also computationally faster, user-friendly and economic compared to other programming languages such as Python or FORTRAN. It allows to produce large amount of databases with good quantitative results. Therefore, simulations were done in MATLAB environment for structure optimization and structural analysis of clusters.

3.1.3. Supercomputers

Since 400 GA runs are performed to find the lowest energy structures, supercomputers with increased speed and high capacity are needed. In this project, supercomputer was supplied by Koç University High Performance Computing Lab. The supercomputer named LUFER was used. This cluster is connected to two servers which are Hattusas and Gordion. Hattusas which consists of 32 nodes with one CPU in each node is used. Since optimization is done for small size of clusters, only 1 node is used.

3.1.4. Avogadro

Avogadro [75] is one of the available software package for visualization and drawing as well as the optimization at classical level. It is free, easy to use and it provides high quality graphical image of structures. Therefore, all graphical figures of structures in this thesis were visualized using the Avogadro software.

3.2. Atomic Simulations at the DFT Level

The DFT approach is used to determine the lowest energy structures of adsorbed hydrogen on each composition of PtCu clusters consisting of 10 atoms. A lot of computational chemistry programs such as Gaussian, SIESTA, DMol3 and NWChem can be used for DFT calculations. In this thesis, Gaussian 09 [76] was used for optimization

at DFT level. Gaussian 09 is worked under supercomputers. Necessary tools for DFT runs are explained below.

3.2.1. Gaussian 09

Gaussian 09 [76] is a computational chemistry program package which is used for geometry optimization by utilizing various approach such as molecular mechanics, ab-initio, DFT, semi-empirical and hybrid methods. The procedure of geometry optimization starts with the calculation of wave function and the energy at a starting geometry and then continues to search a new geometry of a lower energy. This procedure is repeated until the lowest energy geometry is found where the force (first derivative of energy) on each atom with respect to atomic positions is zero. After the optimized condition is reached, several properties can be obtained such as atomic coordinates of optimized molecule, atomic distances and angles, highest and lowest occupied molecular orbitals, mulliken atomic charges and dipole moments.

Frequency calculations are also done to calculate the vibrations of the molecule. Vibrational frequencies are computed by determining the second derivatives of the energy with respect to the atomic positions. Additional to the previously mentioned properties, single point energy, harmonic frequencies, force constants, IR intensities and thermochemical information can be found.

3.2.2. GaussView

GaussView 5.0.9 is one of the visualization programs in computational chemistry. It allows to draw molecules, create inputs files for DFT calculations in Gaussian 09 and graphically examine results obtained in Gaussian 09.

3.2.3. Basis Sets

Basis set is a set of Gaussian functions which describes the shapes of the atomic orbitals. The molecular orbitals are constructed by linear combination of atomic orbitals. DFT calculations require a basis set definition for the system being studied. Basis sets affect the total energy results but it does not guarantee that effect always improves the results. The simplest basis set is known as STO-3G which can work up to thousands atom. Although the STO-3G is the fastest, it is known as least accurate basis set. In our calculations, LANL2DZ basis set which is suitable for heavier atoms like Pt and Cu is used.

3.2.4. Exchange-Correlation (XC) Functional

For the use of DFT, we must know what the form of the exchange and correlation energy functional and introduce the system before start any calculation in Gaussian 09. Exact form of E_{XC} is not known but some sort of approximations are used. Local density approximation (LDA) and generalized gradient approximation (GGA) are the most widely used in DFT. Large number of approximated functionals under these approach with various levels of complexity are available in Gaussian 09. In this thesis, Becke-three parameter hybrid functionals (B3) [77] for exchange part, Perdew-Wang 91 [78] for correlation part were used.

3.2.5. Input File for Gaussian 09

For DFT calculations in Gaussian 09, input script has to be written. The main purpose of the script is to convert atom coordinates to .com file which is necessary extension for Gaussian 09 and used it to calculate total energies of Pt, Cu and Pt-Cu clusters. After optimization, .log file can be obtained from Gaussian 09.

The typical input script which is performed within Gaussian 09 environment consists of the following parts:

(i) Section: defines the name of the checkpoint file (.chk)

(ii) Route Section: specifies the basis set, the theoretical model and the job type

(iii) Title Section: the name of the job

(iv) Charge: specifies the charge of the system

(v) Multiplicity: Spin multiplicity of the system

(vi) Geometry Specification: name of the atoms and their atomic positions (i.e. atomic coordinates)

In Figure 6, created input file for optimization of Pt_{10} cluster in Gaussian 09 can be seen. In this script file, optimization and frequency calculations are done for Pt_{10} cluster using B3PW91 exchange correlation functional and LANL2DZ basis set. Charge is set to 0 while spin multiplicity as doublet.

```
%chk=pt10.chk
# opt freq b3pw91/lanl2dz geom=connectivity

pt10 optimization and frequency

0 2
 Pt                  3.66246919    2.34836636   -0.15743523
 Pt                  2.91694471    0.06438040   -0.03834418
 Pt                  4.17851809   -2.34926027    0.00694396
 Pt                 -0.15943530    2.43671899   -0.01066808
 Pt                 -0.62729729    0.02441245    0.10255229
 Pt                  0.22862254   -2.41026633    0.16461383
 Pt                  2.49190013   -2.49741644    0.07906954
 Pt                 -3.37551305    0.07569710    0.20856954
 Pt                 -2.36097458   -2.39338012    0.26574794
 Pt                  0.08011170   -0.18305525   -1.98219704

 1 2 1.0 4 1.0 5 1.0
 2 3 1.0 7 1.0 5 1.0 10 1.0 4 1.0
 3 7 1.0 5 1.0 10 1.0
 4 10 1.0 8 1.0 5 1.0
 5 10 1.0 8 1.0 9 1.0 6 1.0 7 1.0
 6 9 1.0 7 1.0 8 1.0 10 1.0
 7 10 1.0
 8 9 1.0 10 1.0
 9
 10
```

Figure 6. Input file of Pt_{10} cluster created in GaussView for submission to Gaussian 09

4. RESULTS & DISCUSSION

4.1. The Effect of the Number of GA Runs on Potential Energies

Table 3 shows how many times a structure with the lowest energy was obtained in 100 GA runs for both mono- and bimetallic Pt-Cu clusters consisting of 2-40 atoms. These structures with the lowest energy are not necessarily the same structure for some of the pure and also bimetallic clusters. For example, there are two structures with identical energy for pure Pt clusters with 28 and 40 atoms. Interestingly, there are no Cu clusters that have the same energy but a different structure. All of the bimetallic clusters consisting of 12 or more atoms have at least two structures with the same energy. For both pure and bimetallic clusters, the number of lowest energy structures found for pure Pt and Cu clusters in 100 GA runs was high even for large clusters. However, for PtCu clusters, the number of lowest energy structures in 100 GA runs dramatically decreased when the cluster size increased above 16 atoms.

Gupta potential energies of the lowest energy structures of pure Cu and how many times these lowest energy structures were found in 100 GA runs are presented in Table 3. The lowest potential energy results presented in Table 3 are in good agreement with previous GA study of Cu clusters composed of 56 atoms using the Gupta potential by Darby et al. [48] who used 20 different initial populations and a mutation rate of 0.1. They obtained icosahedron based Cu clusters as the most stable morphology but they did not provide any information either on the number of GA runs or on the number of lowest energy structures. The percentage of runs which gave the lowest energy structures in 100 GA runs for Cu clusters as a function of cluster size are shown in Figure 7 (b). At least 80% of the optimized Cu clusters composed of 2-40 atoms had exactly the same potential energies and structures. This result indicates that 100 GA runs are sufficient to find the

lowest energy structures except for the clusters with 26 and 38 atoms of Cu. Only 28% and 16% of optimized Cu clusters with 26 and 38 atoms, respectively were found as the lowest energy structures.

Table 3. The number of times the lowest energy structures (LES) were found and minimum potential energies for pure Pt and Cu and PtCu clusters composed of 2-40 atoms in 100 GA runs

		Pt		**Cu**		**Pt-Cu**	
N	GA runs	The number of times the LES were found	V_{min}/(eV)	The number of times the LES were found	V_{min}/(eV)	The number of times the LES were found	V_{min}/(eV)
2	100	100	-7.0678	100	-2.5815	100	-4.3502
4	100	100	-17.5520	100	-7.7423	100	-13.0014
6	100	100	-28.0541	100	-13.2377	100	-21.5356
8	100	100	-38.3200	100	-18.6326	37	-30.1452
10	100	99	-48.8217	100	-24.3003	81	-38.7072
12	100	96	-59.1720	100	-30.2780	72	-47.3108
14	100	97	-69.9090	90	-36.2642	20	-55.9608
16	100	99	-80.8188	99	-42.0084	8	-64.5511
18	100	90	-91.4730	99	-47.8513	2	-73.2621
20	100	40	-101.9812	100	-54.0615	5	-81.9759
22	100	95	-112.8747	88	-59.8292	2	-90.6581
24	100	56	-123.6950	83	-65.9368	1	-99.3692
26	100	70	-134.3316	28	-72.0650	1	-108.0607
28	100	68	-145.2589	93	-78.1574	1	-116.8126
30	100	19	-156.2636	99	-84.0125	1	-125.7211
32	100	76	-166.9108	89	-90.2731	1	-134.5578
34	100	24	-177.8761	93	-96.2917	1	-143.3432
36	100	45	-188.6825	58	-102.5018	1	-152.0949
38	100	2	-199.9420	16	-108.9676	1	-161.4103
40	100	29	-210.5891	91	-115.0955	1	-169.9689

The Gupta potential energies of Pt clusters composed of 2-40 atoms and how many times these structures were found in 100 GA runs are shown in Table 3. The lowest potential energies found for Pt clusters are in good agreement with the results from previous studies. Using Gupta potential within GA environment, Oliver Paz-Borbón et al. [62] found the same lowest energy structures with exactly the same potential energy values up to 20 atoms in 100 GA runs. Although we found large number of clusters with the same lowest energy for small Pt clusters (N=2-20 atoms), the number of times the

lowest potential energy found more than 1 time significantly decreased with increasing cluster size. This can be also seen in Figure 7 (a) which is a plot of the percentage of runs for the number of the same lowest energies found in 100 GA runs.

The percentage of runs which gave the lowest energy structures in 100 GA runs for Cu clusters were more than for Pt clusters. This can be perhaps be attributed to the longer bond distance between two Pt atoms compared with Cu atoms (Pt_2=2.66 Å and Cu_2=2.23 Å) which caused an increase in the number of iterations in GA environment to find equilibrium bond distance between each atom within cluster regime.

The lowest Gupta potential energies and how many times these energies were found for PtCu clusters composed of 2-40 atoms are also shown in Table 3. The structures of PtCu composed of 2-6 atoms were in global minima since the same lowest potential energy were found 100 times in 100 GA runs. The percentage of runs which gave the lowest energy of PtCu clusters in 100 GA runs are shown in Figure 8. As seen in Figure 8(a), for small clusters of PtCu up to 10 atoms, all structures obtained as the lowest energy structures were in global minima. For larger clusters consisting of 10 atoms up to 24 atoms the percentage of runs which gave the lowest energy structure sharply decreased with increasing cluster size. It is also obvious to see the trend on remarkable difficulty on finding the lowest energy structures when the cluster is composed of more than 20 atoms. As seen in Figure 8(a), at least 90% of the optimized structures of PtCu clusters consisting of 24-40 atoms, were in local minima. This result shows how the presence of a second metal can dramatically affect the searching performance of GA method.

In order to find out whether structures with a lower energy exist, the number of GA runs was extended up to 400 for each size of cluster. In this systematical work, 200 GA runs for pure Pt and Cu clusters consisting of 2-20 atoms and 400 GA runs for PtCu clusters consisting of 20-40 atoms were made. The Gupta potential energies for the lowest

energy structures found in more than 100 GA runs and how many times these structures were found for pure Pt, Cu and PtCu clusters consisting of 2-40 atoms are shown in Table 4.

For Cu clusters consisting of 2-40 atoms, exactly the same lowest potential energies were obtained both in 100 (see in Table 3) and in more than 100 GA runs (see in Table 4). A comparison of the percentage of runs which gave the lowest energy structures in 100 GA runs and in more than 100 GA runs is given in Figure 7 (b). Since the structures obtained in 100 and more than 100 GA runs had exactly the same energetic and structural properties, 100 GA runs are suggested as a sufficient strategy for predicting the structures of pure Cu clusters consisting of 2-40 atoms.

The lowest potential energies were found for Pt clusters consisting of 2-40 atoms both in 100 (see in Table 3) and in more than 100 GA runs (see in Table 4). A comparison of the percentage of runs which gave the lowest energy structures in 100 GA runs and in more than 100 GA runs is given in Figure 7 (a). Table 4 shows that the potential energies obtained in 400 GA runs were similar with results presented in Table 3 for pure Pt clusters except for Pt_{26} and Pt_{40}. The potential energies of these two specific clusters obtained in 400 GA runs were -134.3332 and -210.6870 eV and were lower than the structures found in 100 GA runs. In 400 GA runs, the lowest energy structures were obtained as 217 times for Pt_{26} and 1 time for Pt_{40}. The minimum energy structures of Pt_{26} and Pt_{40} clusters were obtained for the first time in runs 254 and 225, respectively. The lowest energy structures and the energies of Pt clusters up to 40 atoms matched exactly with the structures presented as global minima by Massen et al. [79] who carried out 1 GA run starting from 30 randomly created individuals.

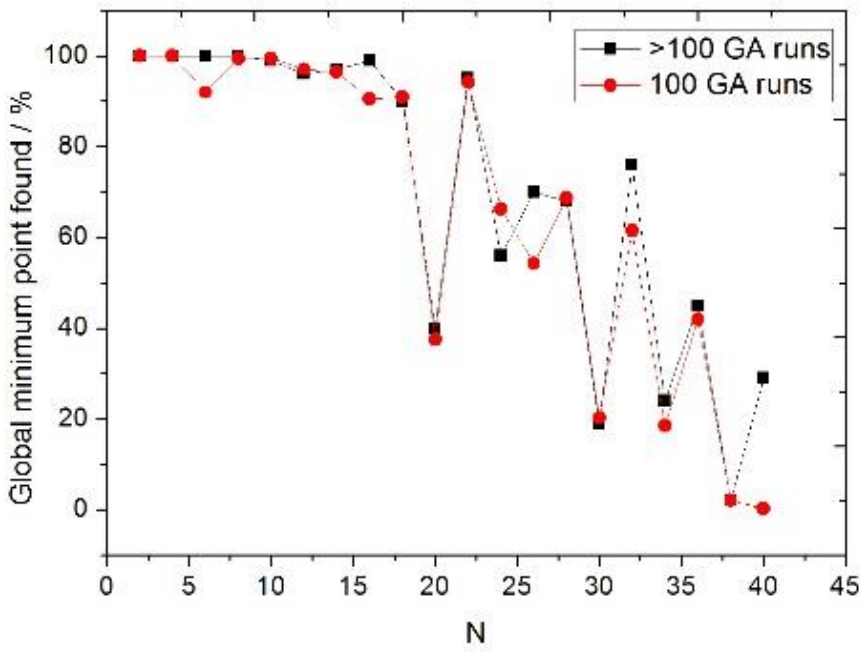

(a) Pt Cluster

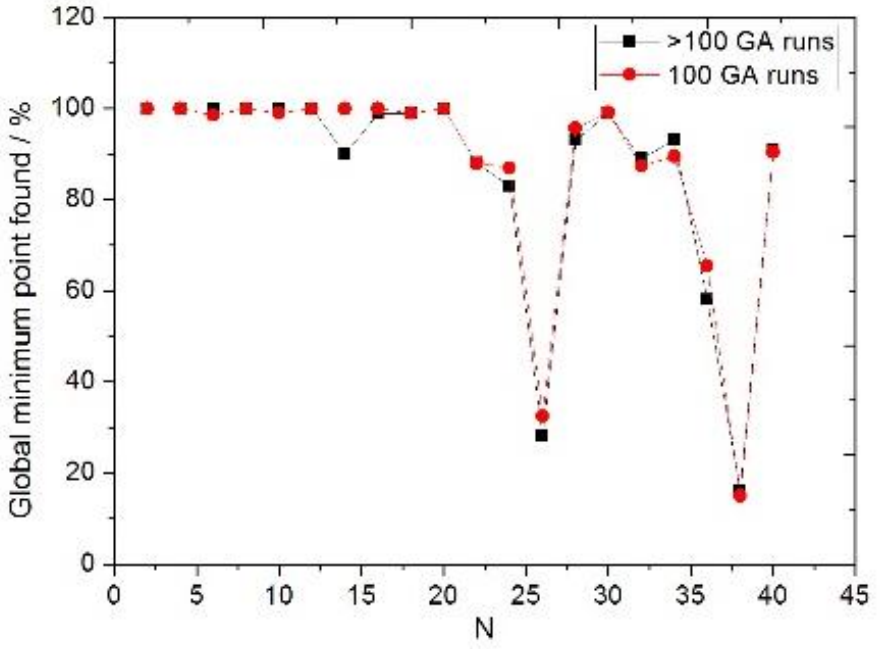

(b) Cu clusters

Figure 7. Percentage of the number of GA runs which gave the lowest potential energy in 100 GA and more than 100 GA runs for Pt (a) and Cu (b) clusters composed of 2-40 atoms

The lowest potential energies found for PtCu clusters in more than 100 GA runs are shown in Table 4. The potential energies obtained in 100 GA runs (see in Table 3) were compared with results presented in Table 4 and the differences in potential energies of various clusters can be seen. Energetically more favorable structures for $Pt_{11}Cu_{11}$, $Pt_{13}Cu_{13}$, $Pt_{14}Cu_{14}$, $Pt_{15}Cu_{15}$, $Pt_{17}Cu_{17}$, $Pt_{19}Cu_{19}$ and $Pt_{20}Cu_{20}$ clusters were discovered when more than 100 GA runs were carried out. This result is also shown in a plot of the percentage of runs which gave the lowest energy structures in 100 GA and more than 100 GA runs for PtCu clusters in Figure 8.

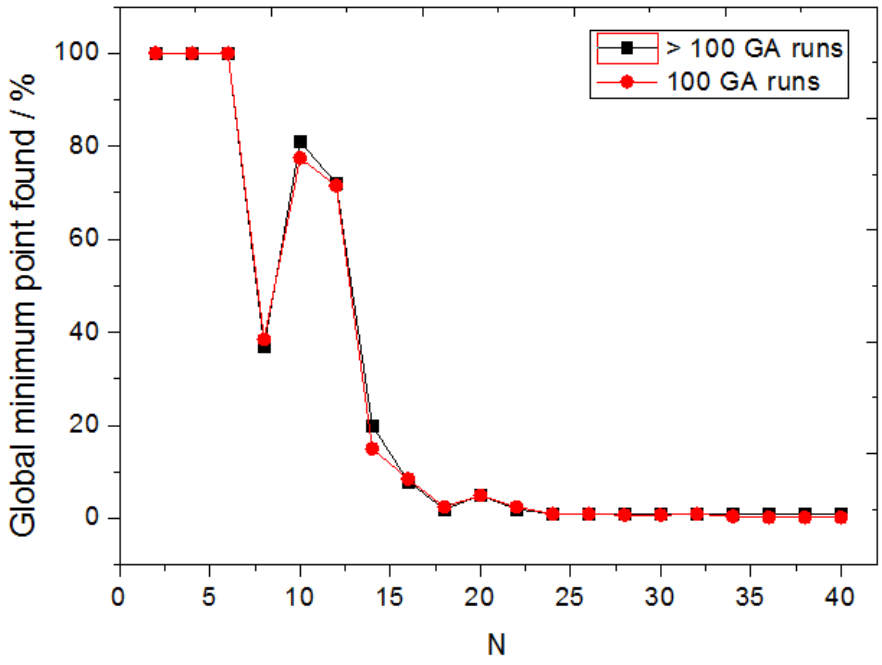

(a) N=2-40 atoms

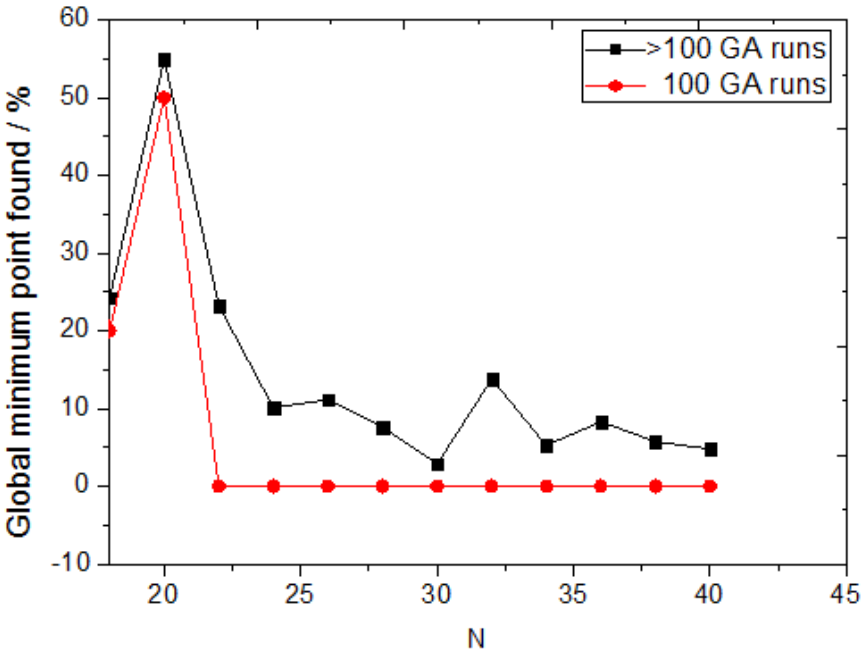

(b) N= 20-40 atoms

Figure 8. Percentage of the number of GA runs which gave the lowest potential energy in 100 GA and more than 100 GA runs for PtCu clusters composed of 2-40 atoms

As seen in Figure 8 (a), the percentage of runs of the number of lowest energy structures found for PtCu clusters significantly decreased when the number of atoms increased. Exactly the same potential energies for clusters composed of 2-24 atoms in both 100 GA and more than 100 GA runs were obtained. However, the finding of global minima of PtCu clusters above 24 atoms were noticeably more difficult due to the large number of possible arrangements and the presence of geometrical isomers and homotops. Results for these specific clusters shown in Table 4 suggest that 100 GA runs starting from 10 candidate solutions (or individuals) are insufficient for determining of the lowest energy morphologies of PtCu clusters and it may cause clusters to locate in local minima.

Table 4. The number of times the lowest energy structures (LES) were found and minimum potential energies for pure Pt and Cu and PtCu clusters composed of 2-40 atoms in more than 100 GA runs

		Pt		**Cu**		**Pt-Cu**	
N	GA runs	The number of times the LES were found	V_{min}/(eV)	The number of times the LES were found	V_{min}/(eV)	The number of times the LES were found	V_{min}/(eV)
2	200	200	-7.0678	200	-2.5815	200	-4.3502
4	200	200	-17.5520	200	-7.7423	200	-13.0014
6	200	184	-28.0541	197	-13.2377	200	-21.5356
8	200	199	-38.3200	200	-18.6326	77	-30.1452
10	200	199	-48.8217	198	-24.3003	155	-38.7072
12	200	194	-59.1720	200	-30.2780	143	-47.3108
14	200	193	-69.9090	200	-36.2642	30	-55.9608
16	200	181	-80.8188	200	-42.0084	17	-64.5511
18	200	182	-91.4730	198	-47.8513	5	-73.2621
20	200	75	-101.9812	200	-54.0615	10	-81.9760
22	400	377	-112.8747	352	-59.8292	10	-90.7297
24	400	265	-123.6950	348	-65.9368	4	-99.3692
26	400	217	-134.3316	130	-72.0650	4	-108.1529
28	400	275	-145.2589	383	-78.1574	3	-116.8569
30	400	81	-156.2636	397	-84.0125	3	-125.7313
32	400	246	-166.9108	350	-90.2731	4	-134.5578
34	400	74	-177.8761	358	-96.2917	2	-143.3673
36	400	168	-188.6825	262	-102.5018	1	-152.0949
38	400	8	-199.9420	60	-108.9676	1	-161.4639
40	400	1	-210.6870	362	-115.0955	1	-170.0549

For pure Pt, Cu and PtCu clusters, the convergence to the lowest energy structures became harder and computing time increased with the increasing number of atoms in clusters. Therefore, increasing computer speed may allow to speed up the initialization and minimize the number of iterations to converge on global minima.

4.2. The Effect of the Number of GA Runs on Cluster Evolution

In this part, the effect of increased number of GA runs on cluster morphologies was investigated. As an example, the evolutionary process of $Pt_{15}Cu_{15}$ cluster with Gupta potential energy changes with increasing number of GA runs is shown in Figure 9.

As illustrated in Figure 89 the atomic arrangement of the initially created structure of $Pt_{15}Cu_{15}$ cluster which was in one of the local minima was irregular (see in Figure 9a). This structure structurally and energetically evolved with increasing number of GA runs. Another local minimum structure was obtained at run 134 (Figure 9b). This structure was more ordered compared to initially created structure. Double-icosahedral based orderly structure was obtained in 396th run (Figure 9c).

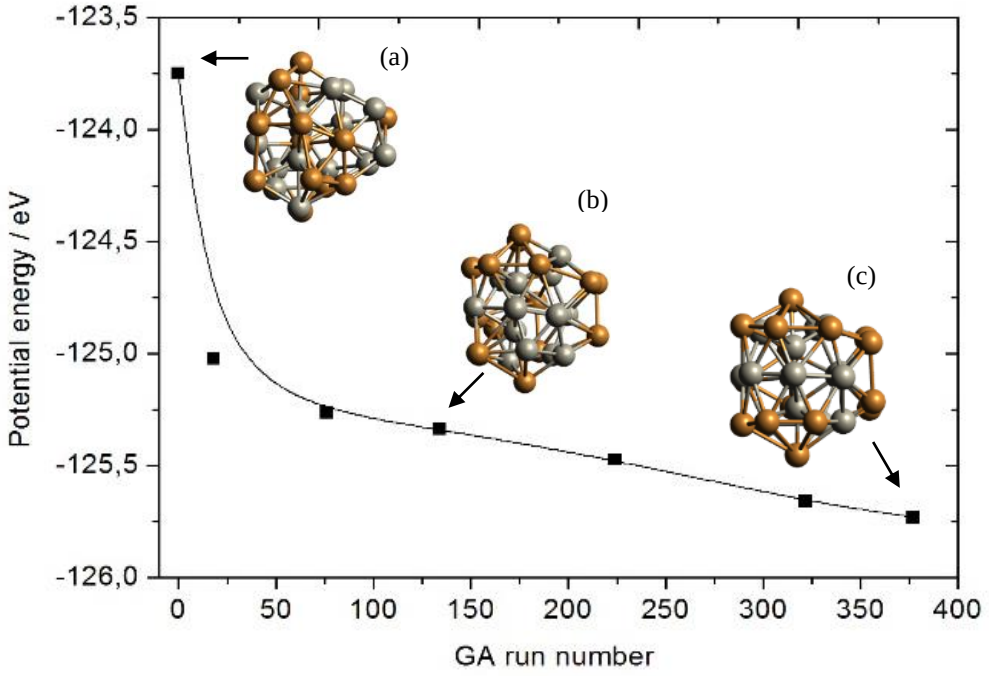

Figure 9. Energetic and structural evolution of $Pt_{15}Cu_{15}$ in GA with the number of GA runs ((a) initially created structure, (b) optimized structure at run 134 (local minima), (c) optimized structure at run 377 (global minima)) (Pt atoms are represented in grey and Cu atoms are represented in yellow)

Further, we noticed the convergence time highly depends on the number of atoms in clusters. Here, results on mean time per run for 2-40 atoms of PtCu clusters are reported starting from structures obtained by different initialization procedure.

In this part, two procedures were followed: (1) optimization of the Gupta potential energy of each size of cluster between 2 and 40 atoms starting from scratch (i.e. randomly generated configurations); (2) optimization of the Gupta potential energy starting from

the previously optimized cluster. In procedure 2, 100 generations for 2 atoms of PtCu clusters were created using randomly initialization code and their atomistic ordering were optimized via Gupta potential energy minimization. Then all global minimum morphologies of 2 atoms were used as initial individuals for 4 atoms of PtCu clusters. 2 more atoms were added to an already optimized cluster and then they were re-optimized. This growth process was proceed up to 40 atoms.

The comparison of average processing time for PtCu clusters of 2-40 atoms based on two different starting points of optimization is seen in Figure 10. Both techniques successfully led to the lowest energy configurations. In small clusters, not only faster computing time but also capturing global minimum morphologies was achieved. However, it is an evident that 1 GA run takes longer time when the cluster size is increased. Convergence time sharply increased especially after 24 atoms.

Importantly in Figure 10, computing speed of algorithm without initialization was shorter than with initialization. Using previously optimized clusters as initial configurations is highly recommended and it would be a computationally more effective searching strategy especially for larger sizes.

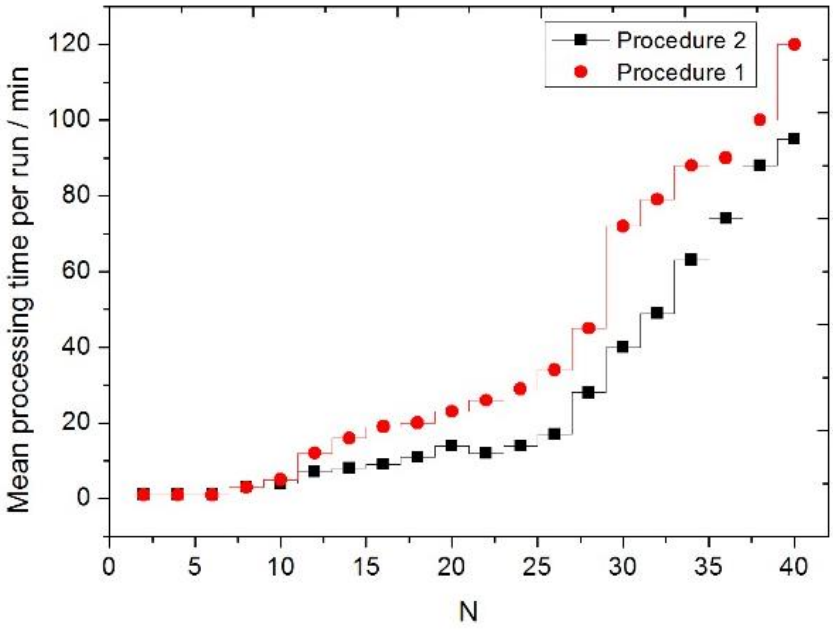

Figure 10. The comparison of average processing time for Pt-Cu clusters of 2-40 atoms based on starting point of optimization (red line represent the mean processing time per run when the optimization starts from randomly initialization, black line represents the mean processing time per run when the optimization starts from the previously optimized cluster size)

4.3. The Effect of the Number of GA runs on DFT Calculations

In this part, the effect of increased number of GA runs on the advanced calculations at DFT level was investigated. As an example, 3 different the lowest energy structures of $Pt_{14}Cu_{14}$ cluster which were obtained in 1 GA, 100 GA runs and in 400 GA runs presented in Figure 11. The potential energy of the lowest energy structure of $Pt_{14}Cu_{14}$ which was found in 1 GA run was -115.750 eV. The potential energy of the lowest energy structure which was found in 100 GA runs at run 82 and in 400 GA runs at run 316 was -116.812 and-116.860 eV, respectively. These structures were fed to DFT environment as an initial structures and optimization and frequency calculations were done using B3PW91 exchange and correlation functional with LANL2DZ basis set in Gaussian 09. After DFT calculations, total energy of each system were found as -4416.815, -4416.870 and -4416.871 in a.u. (Hartrees). It is also seen that calculations at

DFT level to optimization took 31 days for the structure obtained in 1 GA run, 49 days for the structure obtained at run 82 and 14 days for the structure obtained at run 316. This result indicates that distorted structure of Pt-Cu with higher potential energy (see in Figure 11.a) gives higher total energy which is not reliable for stable structures at the end of very long processing time. More regular and ordered initial structures with lower potential energies allows to reach lower total energy at DFT level. The lowest energy structure obtained at run 316 (see in Figure 11c) accelerated DFT calculations and leads more stable structure with better energetic and structural properties.

(a) The lowest energy structure obtained in 1 GA run	(b)The lowest energy structure obtained in 100 GA runs at run 82	(c) The lowest energy structure obtained in 400 GA runs at run 316
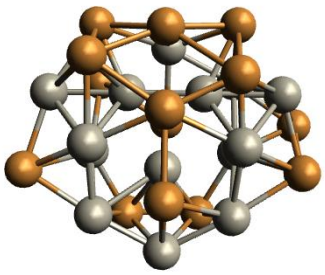	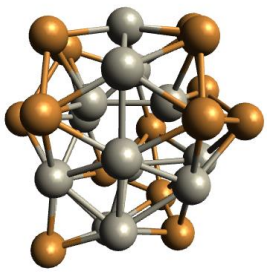	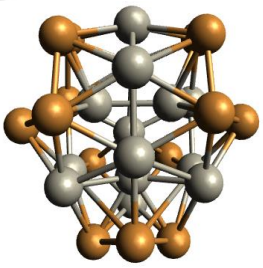
$V_{clus}^{Gupta} = -115.750\ eV$	$V_{clus}^{Gupta} = -116.812\ eV$	$V_{clus}^{Gupta} = -116.860\ eV$
Total energies obtained after DFT calculations in Gaussian 09		
$E_{tot}^{DFT} = -4416.815\ a.u$	$E_{tot}^{DFT} = -4416.870\ a.u$	$E_{tot}^{DFT} = -4416.871\ a.u.$
Job cpu time = 31 days 23 hours	Job cpu time = 49 days 5 hours	Job cpu time = 14 days 9 hours

Figure 11. Energetic, structural and processing time properties of the lowest energy structures obtained in 1 GA run, in 100 GA runs and in 400 GA runs on DFT calculations

In briefly, it can be said that feeding more stable and well-defined structures instead of distorted structures can save processing time and give better properties for further investigations at high level of theory.

4.4. Optimized structures of Pt clusters (N=2-40)

The GM searching procedure for pure Pt clusters was carried out with the following GA input parameters for each GA run; N_{pop} =10; N_{gen} =3; N_{mat} =7; P_{mut} =0.1 with cluster replacement as a mutation operator. The lowest energy structures found for Pt clusters consisting of 2-40 atoms are shown in Figure 12 and their potential energies are listed in Table 5. The lowest energy configurations were reached in 200 GA runs for 2-20 atoms and in 400 GA runs for 22-40 atoms.

Table 5. Accepted the lowest potential energies (V_{min}/eV) obtained in more than 100 GA runs for pure Pt clusters consisting of up to 40 atoms

N	**Pt_N**
2	-7.0678
4	-17.5520
6	-28.0541
8	-38.3200
10	-48.8217
12	-59.1720
14	-69.9090
16	-80.8188
18	-91.4730
20	-101.9812
22	-112.8747
24	-123.6950
26	-134.3316
28	-145.2589
30	-156.2636
32	-166.9108
34	-177.8761
36	-188.6825
38	-199.9420
40	-210.6870

According to the results presented in Figure 12, most of the Pt clusters appeared as regular and symmetric morphology at their lowest energy configurations. The lowest energy structures found for smaller clusters as follows: Pt_4-tetrahedron, Pt_6-tetragonal bipyramid, Pt_8-bicapped octahedron, and Pt_{10}-icosahedron. Pt_{12} was found as an incomplete icosahedron structure in which the atoms at the bottom were nearer to the

cluster center resulting in closed packed structure. Pt_{14} was found as a hexagonal antiprism structure from the family of prismatic uniform polyhedron. Truncated decahedral structures with square-faces were found for Pt clusters consisting of 16<N<24 atoms.

Clusters of 26 and 28 atoms of Pt formed a distorted icosahedron and Pt_{30} formed a 3-fold symmetric icosahedral structure. For clusters with more than 32 atoms, fcc-like closed packed structures were found. Especially for the case of Pt_{38}, perfect fcc-like truncated octahedron (TO) structure was found as the lowest energy structure which is in good agreement with the study was done by Massen et al. [79] who found a TO structure for a cluster with 38 atoms.

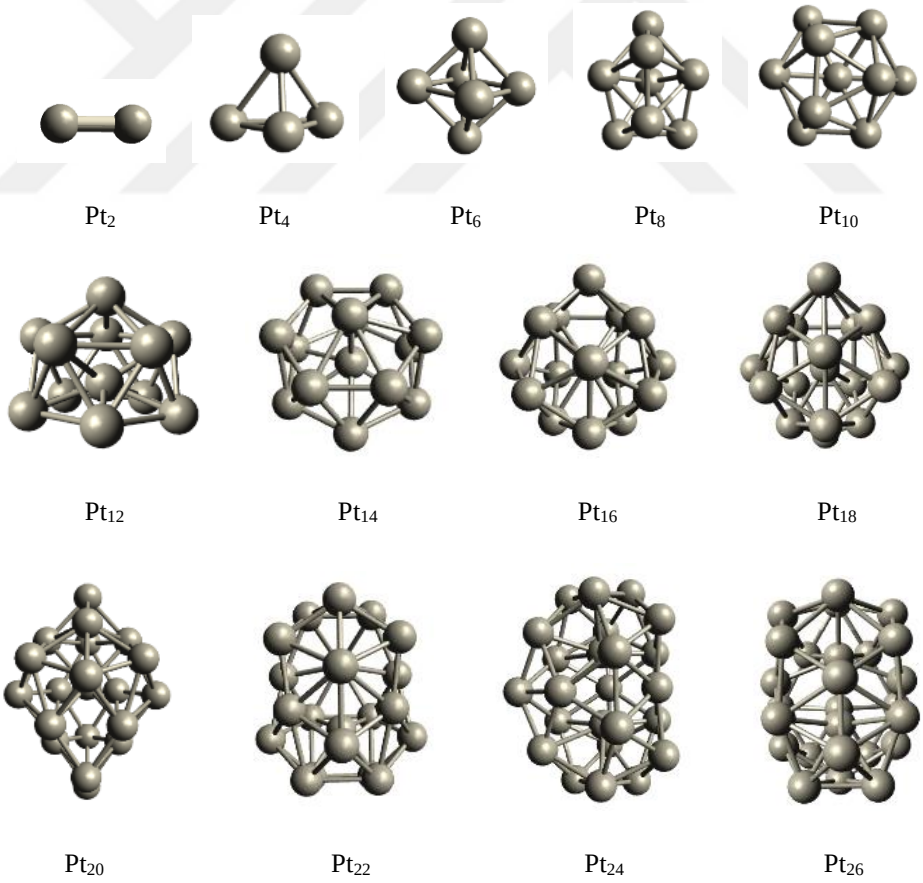

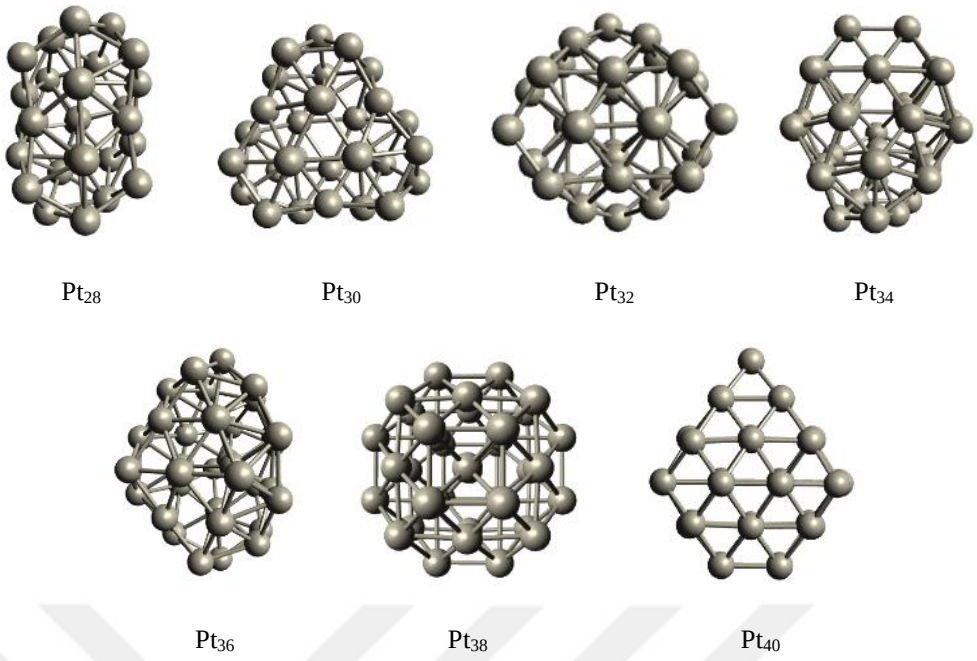

Figure 12. The lowest energy structures of Pt clusters consisting of 2–40 atoms

For Pt_{40} cluster, Tran et al. [80] found that the structure was based on distorted bi-capped TO motif which has 6-atom octahedral core, while in the present study, a more ordered and closed-packed fcc-like structure was found at run 225. This result agreed with the study done by Massen et al. [79] who found a layer by layer fcc-based formation for Pt_{40} cluster.

4.5. Optimized structures of Cu clusters (N=2-40)

The lowest energy structures found for Cu clusters composed of 2-40 atoms, are shown in Figure 13 and their potential energies are listed in Table 6. Same GA input parameters that were used for optimization of Pt clusters were used. The lowest energy configurations were reached in 200 GA runs for 2-20 atoms and in 400 GA runs for 22-40 atoms.

Table 6. Accepted the lowest potential energies (V_{min}/eV) obtained after more than 100 GA runs for pure Cu clusters consisting of up to 40 atoms

N	**Cu_N**
2	-2.5815
4	-7.7423
6	-13.2377
8	-18.6326
10	-24.3003
12	-30.2780
14	-36.2642
16	-42.0084
18	-47.8513
20	-54.0615
22	-59.8292
24	-65.9368
26	-72.0650
28	-78.1574
30	-84.0125
32	-90.2731
34	-96.2917
36	-102.5018
38	-108.9676
40	-115.0955

Although the lowest energy structures of Cu clusters were almost the same structures with Pt clusters for clusters of N=2-10 atoms, bond lengths between Cu atoms were smaller than Pt atoms. Similar to Pt clusters, the most stable morphologies of Cu clusters had symmetric morphology. Most of the Cu clusters and their growing behavior at ground level was based on icosahedron structures. While Cu_{12} was an incomplete icosahedron, complete double icosahedron was achieved at first in Cu_{18} cluster. Cu_{18} grows by adding an atom to the faces since these faces are more open to capture one more Cu atom. A similar growth behavior was observed in a study which was done by Boyukata et al.[81] who investigated the lowest energy structures of pure Cu clusters using MD simulations coupled with effective-pair potential.

Interestingly, the atoms in Cu_{26} were arranged with a similar geometry to Cu_{20} which can be defined as double icosahedron. As the number of atoms in cluster increased, ideal icosahedron structure degenerated.

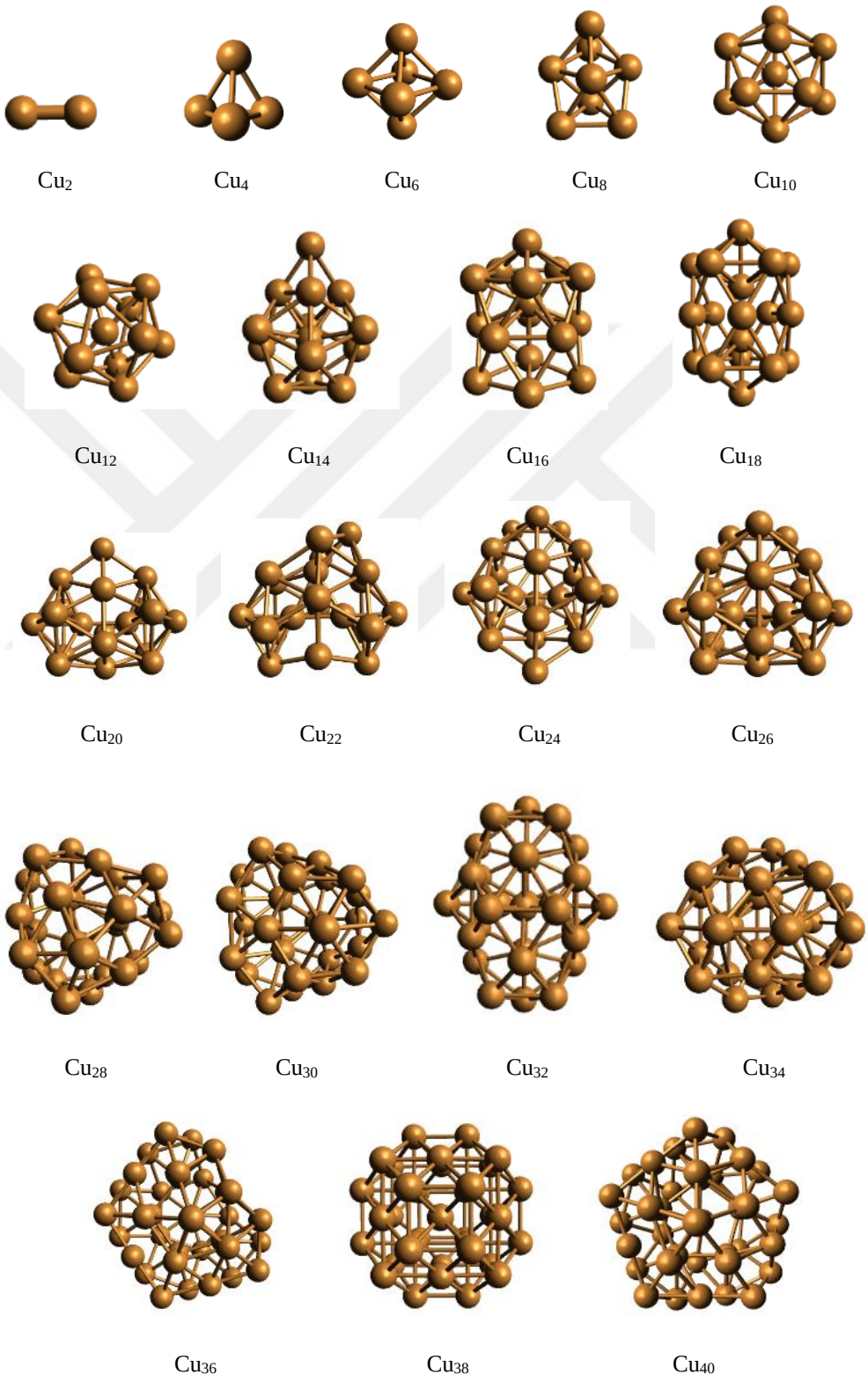

Figure 13. The lowest energy structures of Cu clusters consisting of of 2-40 atoms

For pure Cu clusters with size of 30-40 atoms, Mackay-like structures were observed. Both Cu_{36} and Cu_{40} were in incomplete Mackay structure as a minimum energy configuration. Similar to the pure Pt cluster of 38 atoms, perfect fcc-like TO was obtained for Cu_{38} cluster.

4.6. Optimized structures of PtCu clusters (N=2-40)

The lowest energy structures found for PtCu consisting of 2-40 atoms, are shown in Figure 14 and their potential energies are listed in Table 7. Same GA input parameters were used for optimization of PtCu clusters. The lowest energy configurations were reached in 200 GA runs for 2-20 atoms and in 400 GA runs for 22-40 atoms.

Table 7. Accepted the lowest potential energies (V_{min}/eV) obtained in more than 100 GA runs for PtCu clusters consisting of up to 40 atoms

N	Pt-Cu (z=0.5)
2	-4.35024
4	-13.0014
6	-21.5356
8	-30.1452
10	-38.7072
12	-47.3108
14	-55.9608
16	-64.5511
18	-73.2621
20	-81.9760
22	-90.7297
24	-99.3692
26	-108.1529
28	-116.8569
30	-125.7313
32	-134.5578
34	-143.3673
36	-152.0949
38	-161.4639
40	-170.0549

In the smaller size of PtCu clusters, symmetrical geometries were found as energetically more favorable. The lowest energy structures (at least presumed global minima) of PtCu composed of 4-10 atoms were; Pt_2Cu_2-tetrahedron, Pt_3Cu_3-incomplete

pentagonal prism, Pt_4Cu_4-pentagonal prism with Cu-capped and Pt_5Cu_5-bi-capped pentahedron.

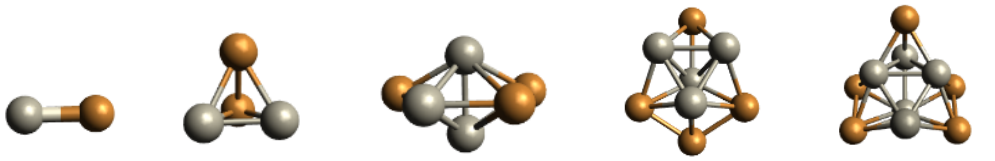

Pt_1Cu_1 Pt_2Cu_2 Pt_3Cu_3 Pt_4Cu_4 Pt_5Cu_5

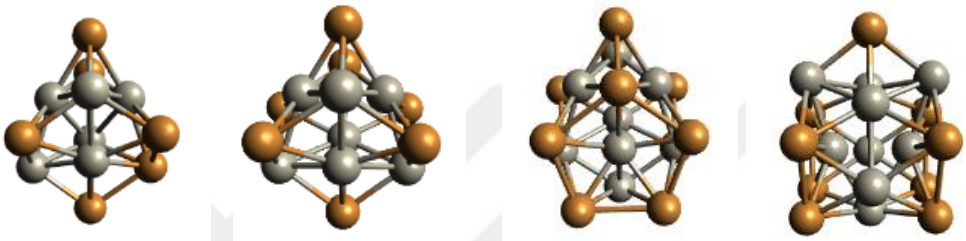

Pt_6Cu_6 Pt_7Cu_7 Pt_8Cu_8 Pt_9Cu_9

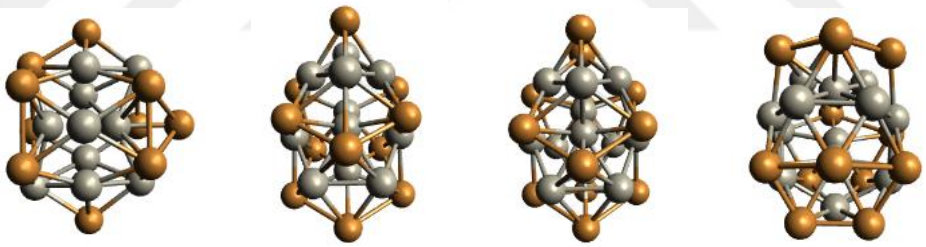

$Pt_{10}Cu_{10}$ $Pt_{11}Cu_{11}$ $Pt_{12}Cu_{12}$ $Pt_{13}Cu_{13}$

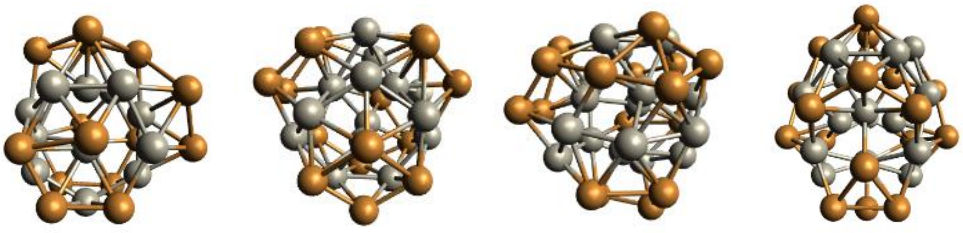

$Pt_{14}Cu_{14}$ $Pt_{15}Cu_{15}$ $Pt_{16}Cu_{16}$ $Pt_{17}Cu_{17}$

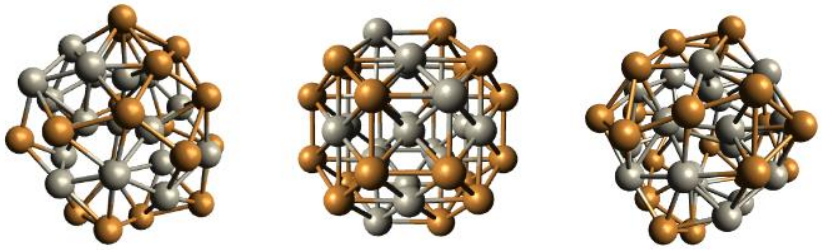

$Pt_{18}Cu_{18}$ $Pt_{19}Cu_{19}$ $Pt_{20}Cu_{20}$

Figure 14. The lowest energy structures of PtCu clusters with 2-40 atoms

Clusters between 12 and 20 atoms, hexagonal anti-prismatic structure with Cu-top atoms was observed. When more atoms were added to the clusters, more distorted double-layer icosahedral structures surrounded by Cu atoms were seen. The perfect fcc-like TO structure for $Pt_{19}Cu_{19}$ cluster was similar to both Pt_{38} and Cu_{38} clusters. Although perfect double layer pentagonal prism was discovered which is similar in structure to Pt_{40} cluster, distorted icosahedron based morphology was found as the lowest energy structure. It was also seen that most of the Cu atoms preferred to bond Pt atoms rather than bond to Cu atoms and cover the Pt surface. This is an obvious result of minimum energy configuration was reached with Pt-Cu bond formation without segregation.

4.6.1. Homotop structures of PtCu clusters

Previously in Section 4.1, we showed that the percentage of runs which gave the lowest energy structures of PtCu clusters sharply decreased with increasing number of atoms due to the significant effect of the large number of possible isomers and homotops. Through the searching cycles for optimum structures, some homotopic structures for some specific cluster sizes were investigated. These homotopic structures had the same potential energies but differed in the two or more-atom position. The homotopic structures found for PtCu clusters consisting of 12, 20, 26, 28 and 34 atoms are shown in Figure 15.

The lowest energy homotops found at the Gupta level for PtCu clusters showed that most of the Cu atoms have a tendency to segregate to the surface. Our calculations cannot quantitatively determine which of the homotops (see in Figure 15) provide the lowest energy structure. Therefore these specific structures were defined as presumed global minima and have to be confirmed at a higher level of theory such as relaxation in DFT environment.

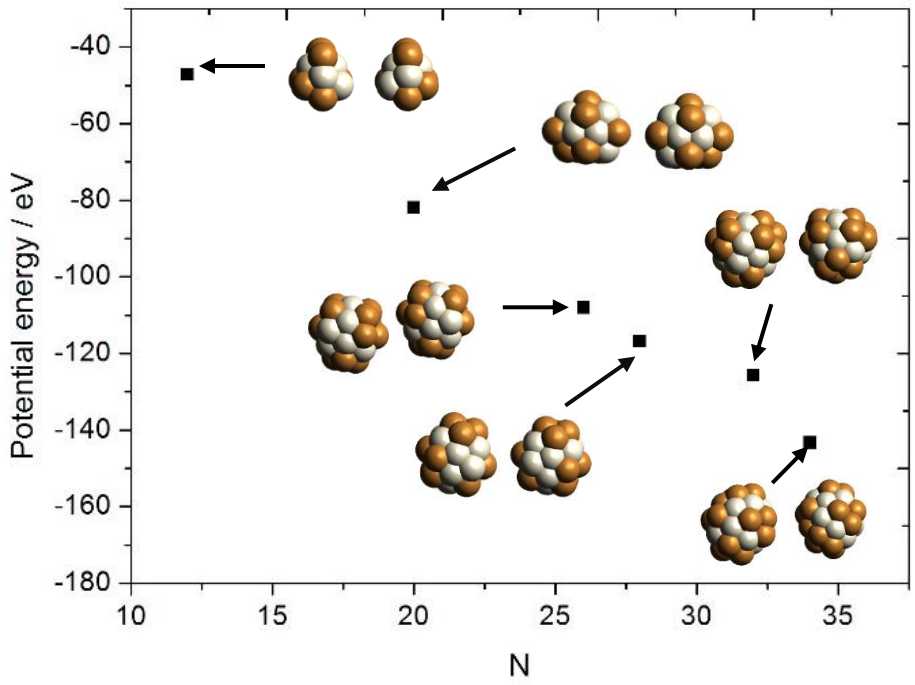

Figure 15. Potential energies and morphologies of homotopic structures for PtCu clusters composed of 12, 20, 26, 28 and 34 atoms

The 2D views of homotopic structures of $Pt_{10}Cu_{10}$ and $Pt_{14}Cu_{14}$ together with their 3D views are presented in Figure 16. The clusters in first column are homotops and in the second column, they are atomic arrangements in 2D. Results in Figure 16 pointed out that atomic arrangements can be different while the potential energies are the same.

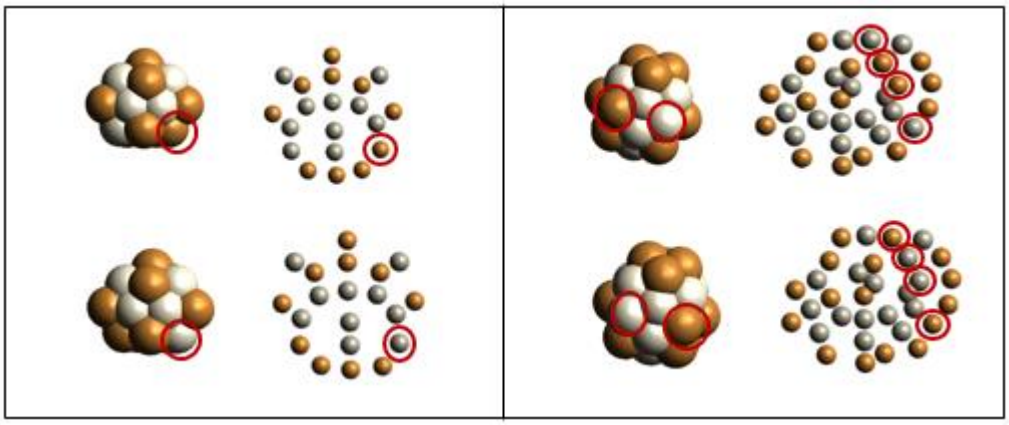

(a) $Pt_{10}Cu_{10}$ (b) $Pt_{14}Cu_{14}$

Figure 16. Two homotops for the $Pt_{10}Cu_{10}$ cluster is in the left and for $Pt_{14}Cu_{14}$ is in the right. First column in both side showed the homotops in 3D while second column in 2D arrangements.

4.7. Energetic Analysis of Pt, Cu and PtCu Clusters

4.7.1. Binding Energy

Binding energy of optimized clusters of pure Pt, Cu and PtCu clusters consisting of up to 40 atoms were calculated using Eq 2.9. Fig. 17 shows the binding energies of Pt clusters (black line) calculated at the Gupta level, Cu clusters with N=2-40 atoms (red line) as well as the corresponding binding energies of optimized PtCu (blue line) and arithmetically averaged binding energies of PtCu (yellow line).

The calculated binding energies of pure Pt (black line) and Cu clusters (red line) with N = 2–40 atoms shows that optimized Pt and Cu clusters were energetically favorable as the binding energy per atom was positive for all cluster sizes. It can be also seen that binding energy slightly increased when cluster become larger.

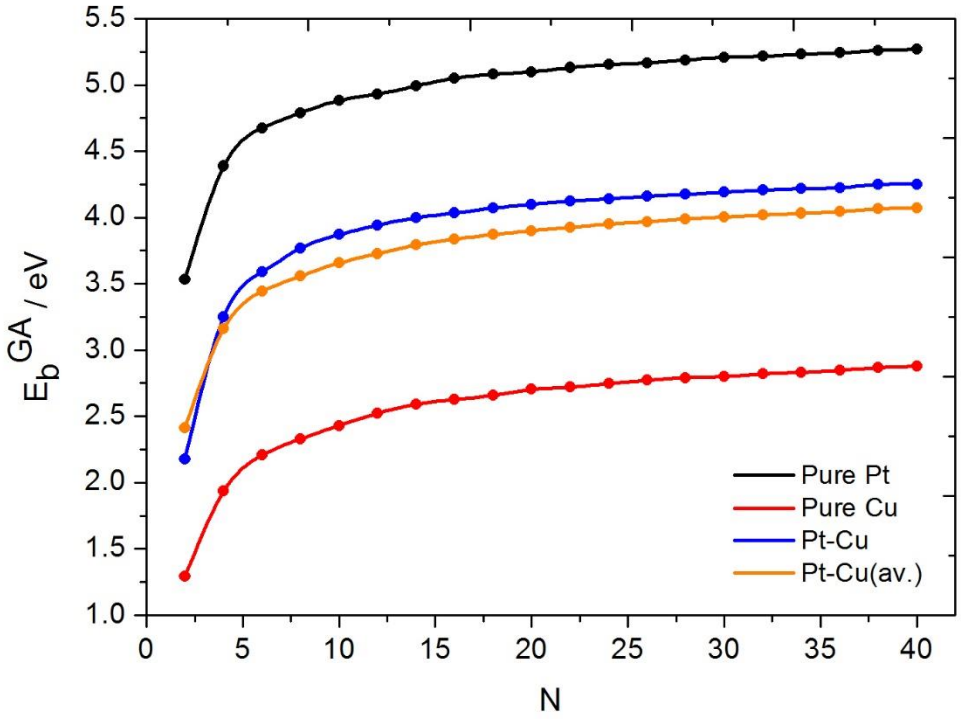

Figure 17. GA binding energies for pure Pt, Cu and Pt-Cu clusters with N=2-40 atoms

From Figure 17, it is also seen that calculated binding energies for optimized clusters of PtCu clusters (N=2-40) (blue line) lie slightly above the arithmetical average of binding energies of their pure counterparts (yellow line). It is also apparent the binding energies of calculated PtCu clusters are closer to the binding energies of Pt rather than Cu clusters.

4.7.2. Excess Energy

The calculated excess energies of PtCu clusters (N=2-40) at Gupta level for both local minima and presumed global minima (black line) are shown in Figure 18. Excess energies for each cluster size were obtained as a negative which indicates that our optimized PtCu clusters were energetically favorable. The most negative excess energy was obtained from the structure where the lowest potential energy was found.

Additionally, the more negative excess energy increased dramatically as the number of atoms increased and it reached the smallest value for the largest cluster which is $Pt_{20}Cu_{20}$.

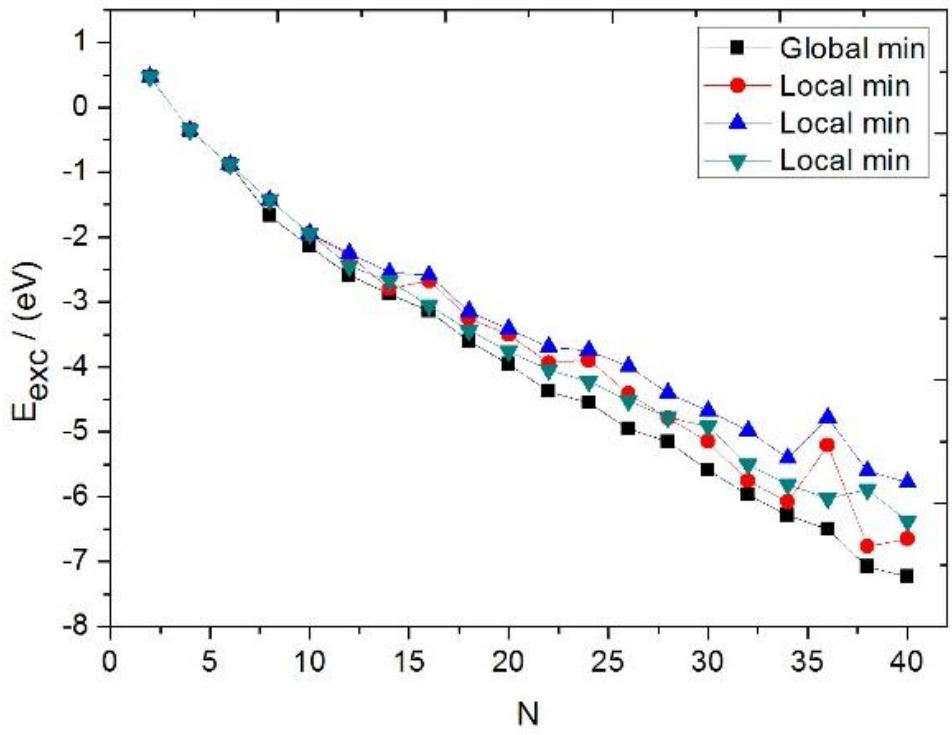

Figure 18. GA excess energies of local and global minima for PtCu clusters with N=2-40 atoms

4.7.3. Second Difference in Energy

Second difference in energy which is another important way to measure the relative stability of each composition with respect to its neighbors is calculated using Eq. 2.11. To determine the Gupta potential energies of neighbors of PtCu clusters up to 40 atoms, same procedure of GA optimization with the large number of runs was applied. The number of GA runs and potential energy results of optimized neighboring compositions are presented in Table 8.

Table 8. Potential energy (eV) values of optimized neighboring compositions of PtCu clusters (N=2-40 atoms)

Structure	Neighboring compositions	Potential energy (eV)	The number of GA runs
Pt_1Cu_1	Pt_2	-7.0678	100
	Cu_2	-2.5815	100
Pt_2Cu_2	Pt_3Cu_1	-16.2444	100
	Pt_1Cu_3	-8.8660	100
Pt_3Cu_3	Pt_4Cu_2	-24.8651	100
	Pt_2Cu_4	-17.6863	100
Pt_4Cu_4	Pt_5Cu_3	-33.4008	100
	Pt_3Cu_5	-26.3601	100
Pt_5Cu_5	Pt_6Cu_4	-41.9895	100
	Pt_4Cu_6	-35.1800	100
Pt_6Cu_6	Pt_7Cu_5	-50.5657	100
	Pt_5Cu_7	-43.8220	100
Pt_7Cu_7	Pt_8Cu_6	-59.3730	100
	Pt_6Cu_8	-52.4470	100
Pt_8Cu_8	Pt_9Cu_7	-67.8594	100
	Pt_7Cu_9	-61.1530	100
Pt_9Cu_9	$Pt_{10}Cu_8$	-76.6250	100
	Pt_8Cu_{10}	-69.8970	100
$Pt_{10}Cu_{10}$	$Pt_{11}Cu_9$	-85.2685	400
	Pt_9Cu_{11}	-78.5858	400
$Pt_{11}Cu_{11}$	$Pt_{12}Cu_{10}$	-93.9791	400
	$Pt_{10}Cu_{12}$	-87.3428	400
$Pt_{12}Cu_{12}$	$Pt_{13}Cu_{11}$	-102.6568	400
	$Pt_{11}Cu_{13}$	-96.0052	400
$Pt_{13}Cu_{13}$	$Pt_{14}Cu_{12}$	-111.4017	400
	$Pt_{12}Cu_{14}$	-104.8220	400
$Pt_{14}Cu_{14}$	$Pt_{15}Cu_{13}$	-120.1449	400
	$Pt_{13}Cu_{15}$	-113.4901	400
$Pt_{15}Cu_{15}$	$Pt_{16}Cu_{14}$	-129.0871	400
	$Pt_{14}Cu_{16}$	-122.3148	400
$Pt_{16}Cu_{16}$	$Pt_{17}Cu_{15}$	-137.8625	400
	$Pt_{15}Cu_{17}$	-131.0696	400
$Pt_{17}Cu_{17}$	$Pt_{18}Cu_{16}$	-146.6719	400
	$Pt_{16}Cu_{18}$	-139.9602	400
$Pt_{18}Cu_{18}$	$Pt_{19}Cu_{17}$	-155.4805	400
	$Pt_{17}Cu_{19}$	-154.6590	400
$Pt_{19}Cu_{19}$	$Pt_{20}Cu_{18}$	-164.1647	400
	$Pt_{18}Cu_{20}$	-158.0769	400
$Pt_{20}Cu_{20}$	$Pt_{21}Cu_{19}$	-173.2751	400
	$Pt_{19}Cu_{21}$	-166.6218	400

Figure 19 is a plot of the second difference in energy for PtCu clusters between N = 2 - 40 which is another important way to measure the relative stability of each composition with respect to its neighbors. From Figure 18, it is remarkably seen that PtCu cluster with 38 atoms has the highest relative stability. This result is another evidence which shows that fcc-like truncated octahedron is the most stable structure for 38 atoms which is in good agreement with the study was done by Calvo and Yurtsever [64] .

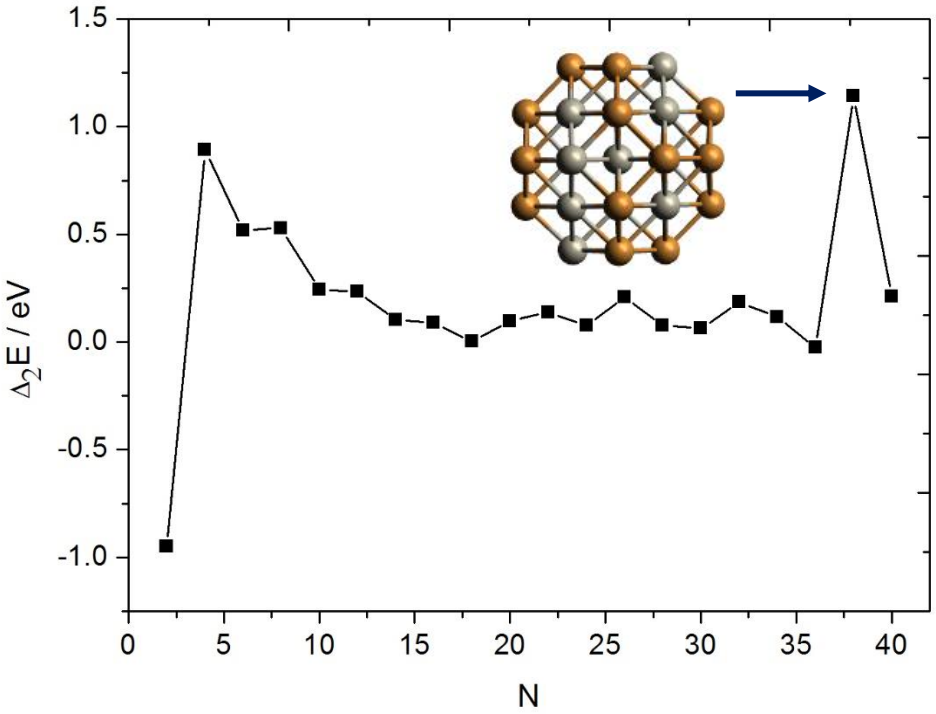

Figure 19. Second difference in energy for PtCu clusters (N=2-40 atoms) at the Gupta potential level

4.8. Structural Analysis of Pt, Cu and PtCu Clusters

4.8.1. Average Weighted Bond Length

For a detailed structural analysis of the lowest energy morphologies, average bond lengths, ECN values and second order parameters were calculated for PtCu clusters up to 40 atoms. Calculated average bond lengths of pure Pt, Cu and PtCu clusters are shown in Figure 20. It is seen that the average bond lengths of Pt, Cu and PtCu clusters generally increase as cluster size increases up to 40 atoms. Cu_{26}, Cu_{28} and $Pt_{13}Cu_{13}$, $Pt_{15}Cu_{15}$ and

$Pt_{18}Cu_{18}$ clusters deviate from this trend since these clusters are more distorted and less symmetric compared to clusters below 26 atoms.

Average bond lengths of Pt-Pt are higher than average bond lengths of Cu-Cu due to the longer bond distance of Pt_2 (2.66 Å) compared to Cu_2 (2.23 Å) which were calculated at DFT level using spin unrestricted B3PW91 exchange correlation functional and LANL2DZ basis set in Gaussian 09 [76].

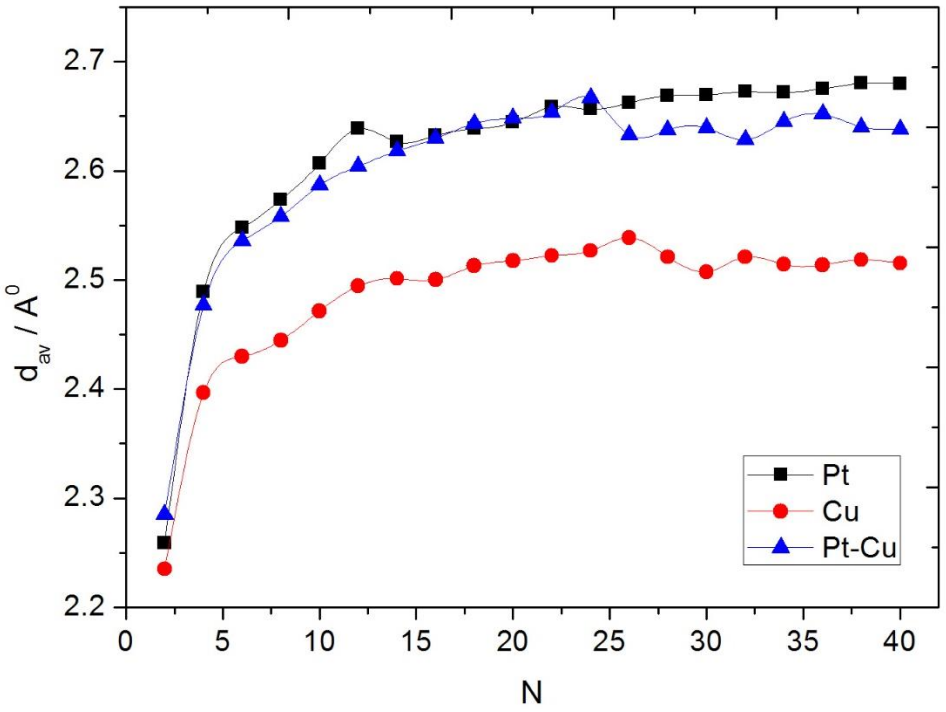

Figure 20. Calculated average bond lengths for pure Pt, Cu and Pt-Cu clusters consisting of 2-40 atoms

4.8.2. Effective coordination number of Pt, Cu and PtCu clusters

The average values of bond lengths were used to calculate effective coordination number of each atom (ECN_i) in Pt, Cu and PtCu clusters. Averaged ECN values of Pt, Cu and PtCu clusters consisting of 2-40 atoms were also calculated and presented in Figure 21. ECN values of Pt clusters were lower than Cu clusters and PtCu clusters had ECN values in between ECN values of pure Pt and Cu clusters. Figure 21 indicates that ECN values increased when cluster size increased for both mono and bimetallic clusters.

However, ECN values decreased especially for clusters of Cu_{28}, Cu_{30}, Cu_{34}, Cu_{36}, Pt_{28}, $Pt_{13}Cu_{13}$, $Pt_{14}Cu_{14}$ and $Pt_{15}Cu_{15}$ since more distorted atomic ordering was seen.

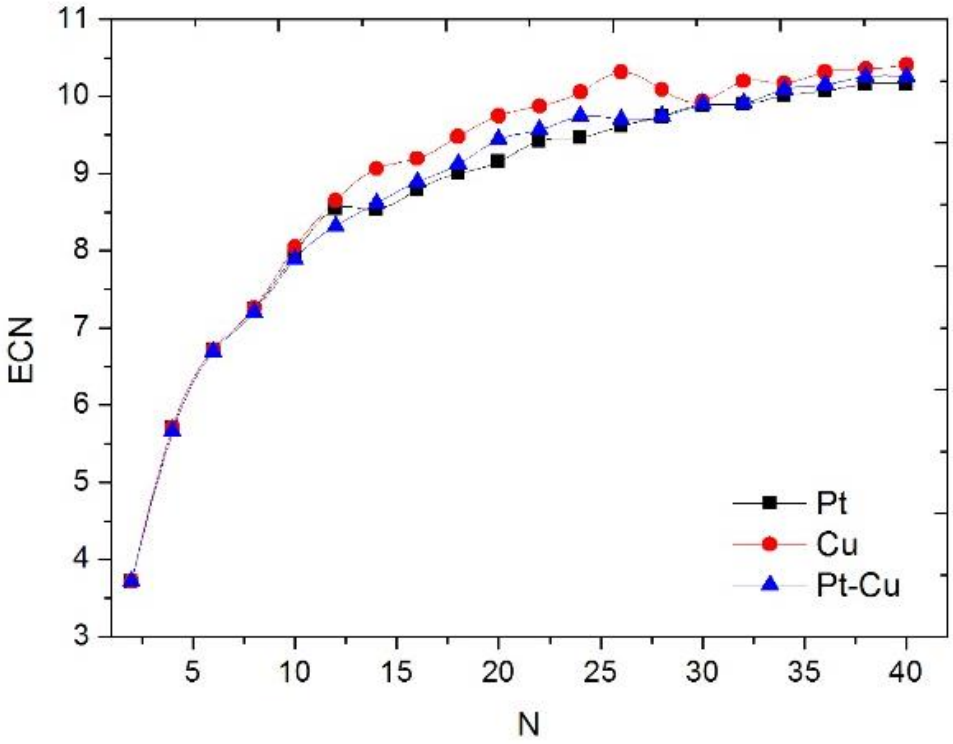

Figure 21. ECN values of Pt, Cu and PtCu clusters (N=2-40 atoms)

4.8.3. Second order parameter

Second order parameter (σ) was needed to distinguish which homo- or hetero-bond dominates to the lowest energy structures. Avogadro [82] which is the computational chemistry program package was used in visualization and counting the number of Pt-Pt, Pt-Cu and Cu-Cu bonds in Pt-Cu clusters to calculate σ using Equation 2.14. Figure 22 shows the calculated σ values for PtCu clusters consisting of 2-40 atoms.

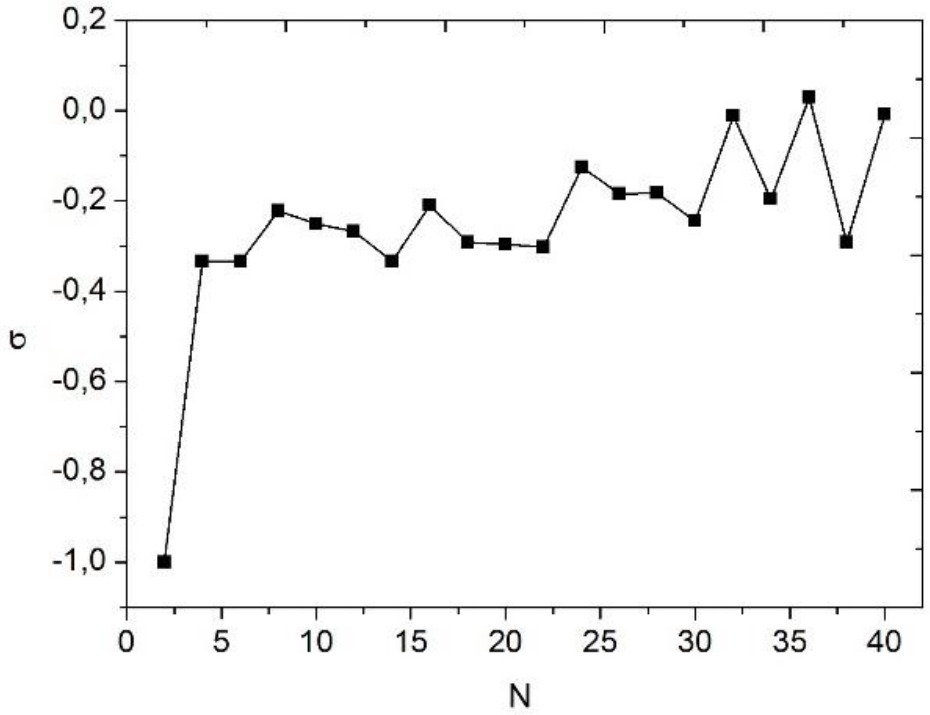

Figure 22. Second order parameter (σ) for PtCu clusters consisting of 2-40 atoms

As we mentioned in Structural Analysis (see in Section 2.4.5.), a negative second order parameter indicates that clusters are mixed (e.g. σ=-1, complete mixing). From our analysis on the number of the Pt-Pt, Cu-Cu and Pt-Cu bonds, the number of Pt-Pt and Pt-Cu bonds were found to be more than Cu-Cu bonds due to the presence of strong binding energy of Pt atoms presented in Figure 17 (black line). As clearly seen in clusters above 28 atoms (see in Figure 13) Cu atoms preferred to bind Pt atoms where located in core region and this resulted in an increase of the number of Pt-Cu bonds. Our results indicated that all morphologies at ground level were in their mixed forms. The two lowest σ values were found for Pt_7Cu_7 and $Pt_{19}Cu_{19}$ clusters which are -0.33 and -0.29, respectively. Although the lowest energy configurations were mixed, they are still far away from being perfectly mixed (i.e. σ = -1)

4.9. DFT Optimization of PtCu Clusters

In this part, each composition of 10 atoms of PtCu clusters were optimized at the DFT level using B3PW91 functional and LANL2DZ basis set. Initial configurations were created with GA coupled with Gupta potential. Optimized morphologies and their total energies (a.u. in Hartrees) are showed in Figure 23.

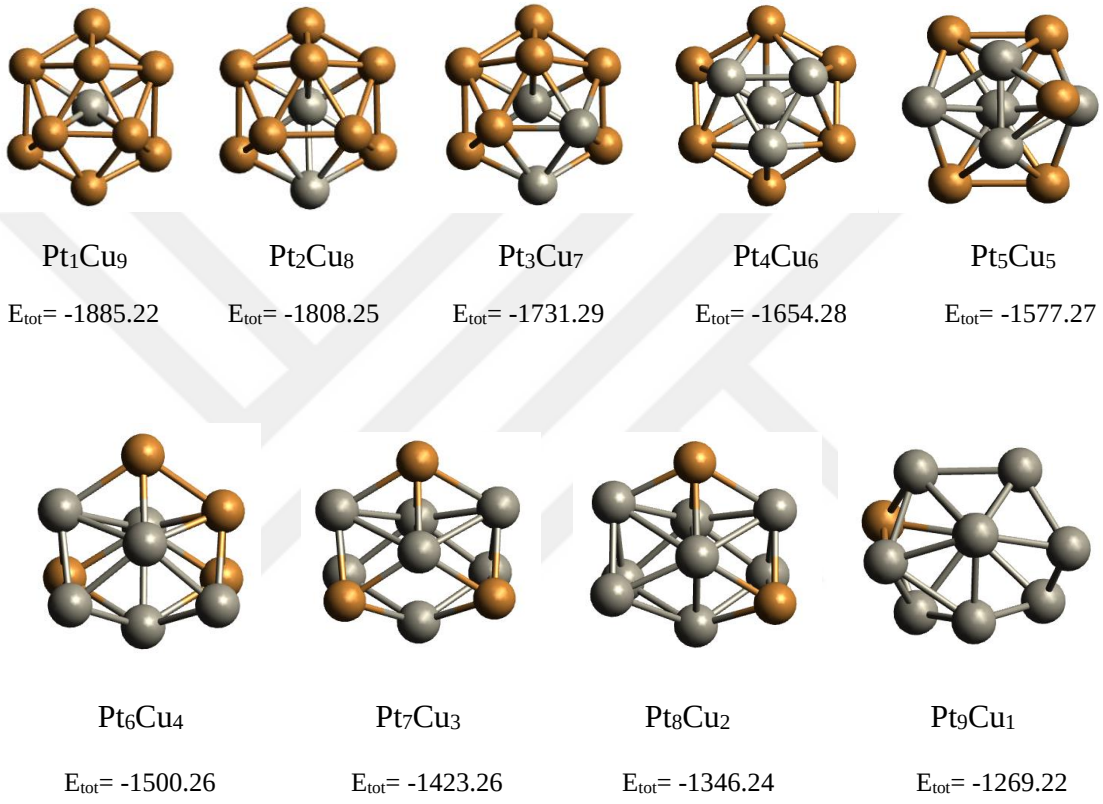

Figure 23. Optimized structures and total energies of each composition of 10 atoms of PtCu clusters at DFT level

Cu-rich clusters showed high symmetric and ordered morphologies. When the number of Pt atoms increased in the clusters, structures became distorted and more relaxed (see in 2nd row in Figure 23).

4.9.1. Energetic Analysis

To determine which composition is energetically favorable, excess energy (i.e. exothermicity of mixing) was calculated. Excess energies of optimized clusters are shown in Figure 24.

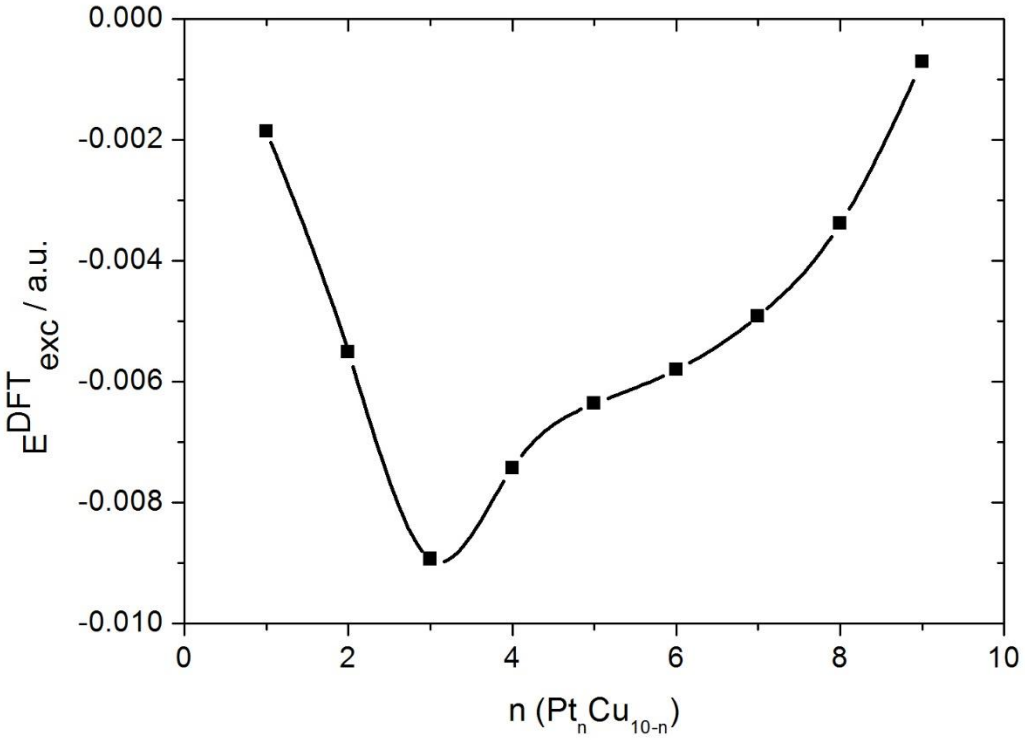

Figure 24. DFT excess energies as a function of Pt atoms in the Pt_nCu_{10-n}

As it seen in Figure 24, dynamical instability increases when the number of Pt atoms increases. It reaches the highest potential energy which is unfavorable with Pt_9Cu_1 cluster. Importantly, energetically more stable configuration was reached with the atomic composition of 3:7 of PtCu cluster.

4.9.2. Structural Analysis

Average bond lengths of each composition of PtCu clusters consisting of 10 atoms are presented in Figure 25. It is seen that average weighted bond lengths increases with the Pt composition in PtCu cluster which is in a good agreement with our findings showed

that average bond length of Pt_{10} cluster is longer than Cu_{10} cluster which are 2.6464 and 2.5376 Å, respectively.

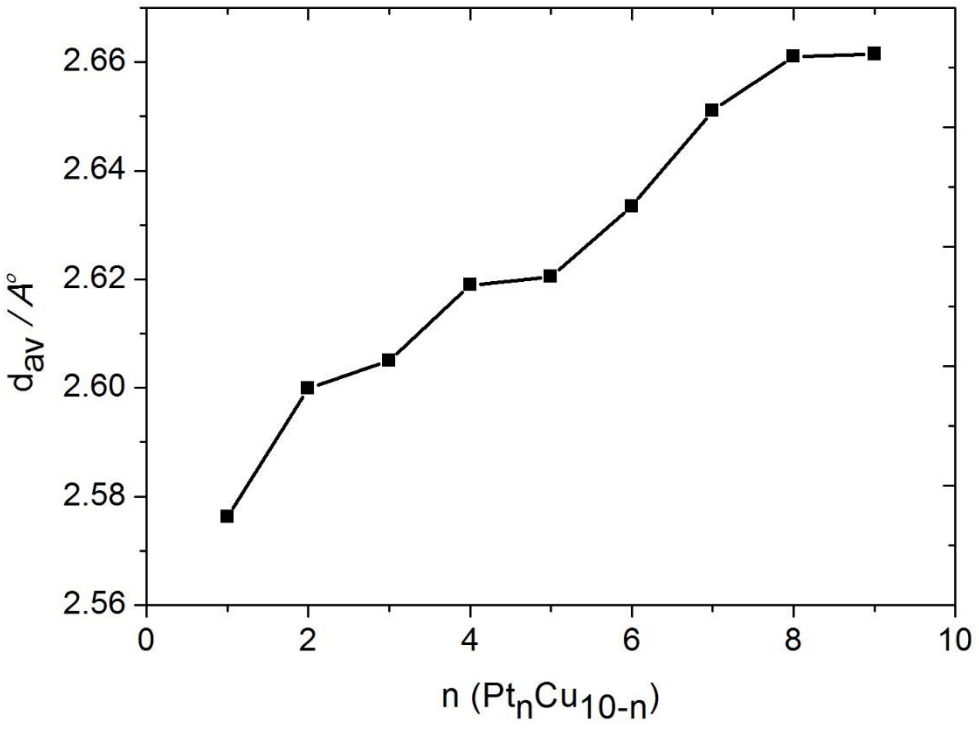

Figure 25. Calculated average bond lengths as a function of Pt atoms in the Pt_nCu_{10-n} cluster

ECN values was also calculated using average bond lengths and are shown in Figure 26. It is well known that bulk Pt and Cu clusters have similar face-centered cubic structures. Our findings on ECN of Pt_{10} and Cu_{10} clusters showed that Pt_{10} has lower ECN than Cu_{10} which are 4.3375 and 5.3437, respectively. We expected that ECN values of each composition of 10 atoms of PtCu clusters would have in between pure Pt_{10} and Cu_{10} clusters. As seen in Figure 26, our calculated ECN values of each composition of 10 atoms of PtCu clusters were optimized at DFT level are in between ECN values of pure Pt and Cu cluster consisting of 10 atoms. Results also show that Pt-rich clusters have lower ECN than Cu-rich clusters.

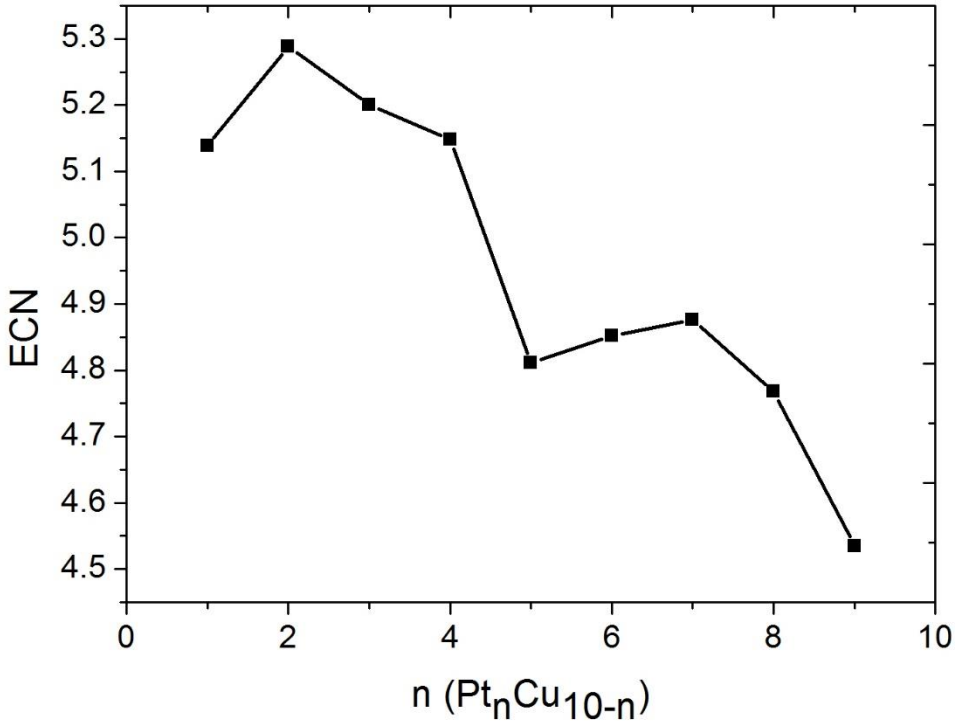

Figure 26. ECN as a function of Pt atoms in the Pt_nCu_{10-n} cluster

4.9.3. Electronic Analysis

Detachment energy (DE) and ionization potential (IP) are another two important quantities to improve our understanding on reactivity of clusters. Calculated DE and IP values are shown in Figure 27. Our results show that IP slightly increases with the number of Pt atoms in clusters while Pt amount causes the oscillations for DE results. It can be also seen that IP has higher values than DE which indicates that it is more difficult to remove one electron than add one electron to the system.

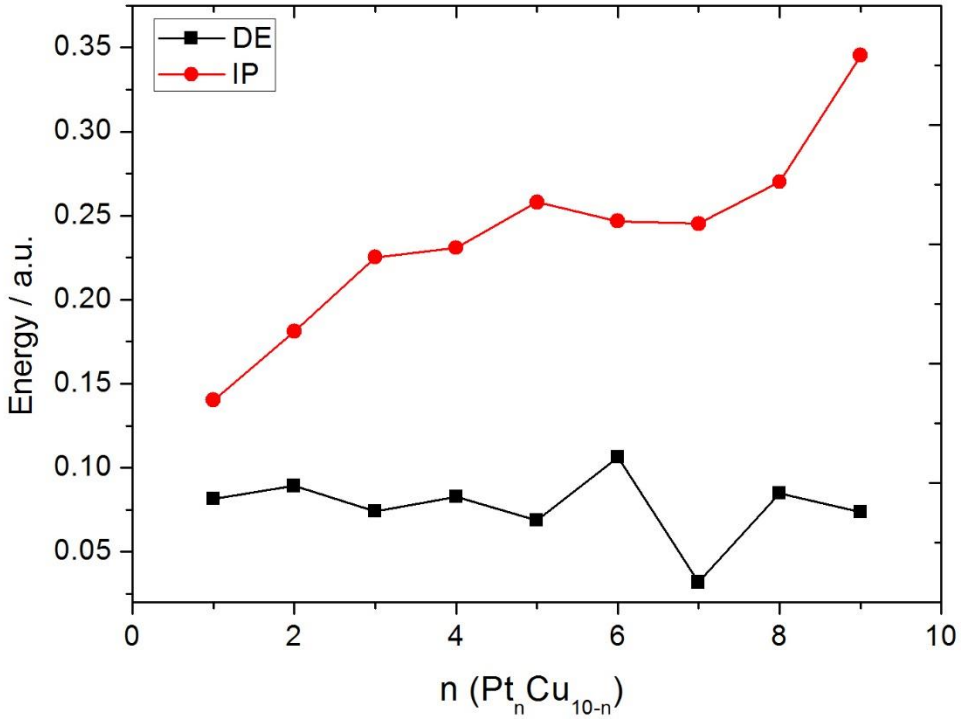

Figure 27. Detachment energy and ionization potential as a function of Pt atoms in the Pt_nCu_{10-n}

4.10. Adsorption Study at DFT Level

It has been noted that PtCu clusters are much more efficient catalysts for oxygen reduction reaction than pure element clusters [16, 83]. In order to improve atomistic understanding on the activity, one hydrogen atom and OH molecule were adsorbed separately to pure Pt, Cu and Pt_3Cu_7 cluster which is energetically most favorable composition of 10 atoms of PtCu in different charge states such as cationic, anionic and neutral. Further, hydrogen adsorption on pure Pt, Cu and Pt_3Cu_7 clusters from different sites such as top, bridge and hollow was studied.

4.10.1. Pt Cluster with H atom and OH Molecule

Global optimization of Pt_{10} cluster involving one hydrogen atom and OH molecule separately was done at DFT level using Gaussian 09. LANL2DZ basis set and B3PW91 functional was used in the calculations.

4.10.1.1. Adsorption Properties of H and OH on Pt_{10} Cluster in Different Charge States

Figure 28 shows the ground state structures and total energies of Pt_{10} cluster with adsorbed hydrogen atom and OH molecule in the different charge states, namely anionic, cationic and neutral. Charge states were considered for the system which consists of metal and adsorbed species. Optimization were performed without freezing the structures.

	Neutral $(Pt_{10}/H)^0$	**Anionic** $(Pt_{10}/H)^-$	**Cationic** $(Pt_{10}/H)^+$
Pt_{10} / H	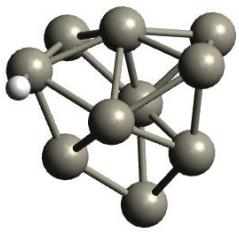	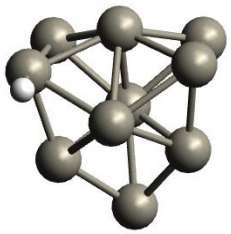	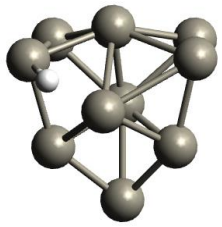
E_{tot} / a.u.	-1192.8325	-1192.9430	-1192.5665
	Neutral $(Pt_{10}/OH)^0$	**Anionic** $(Pt_{10}/OH)^-$	**Cationic** $(Pt_{10}/OH)^+$
Pt_{10} / OH	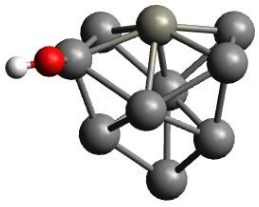	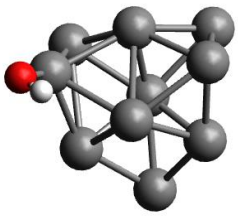	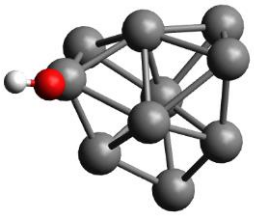
E_{tot} / a.u.	-1268.023	-1268.1445	-1267.7544

Figure 28. The lowest energy structures and total energies of adsorbed H and OH on Pt_{10} cluster in neutral, anionic and cationic charge states (Pt is represented by grey and hydrogen is white while oxygen is represented by red)

From these structures, it can be seen that both hydrogen atom and OH molecule preferred to bond at the top site of Pt atom. Angle between H and Pt atom was obtained

as 180^0. Similarly, the angle between O and Pt atom was 180^0 and the angle of H-O-Pt system is nearly 120^0. Further, adsorption energies and properties of Pt_{10} / H and Pt_{10} / OH systems are summarized in Table 9.

Table 9. Adsorption properties of H and OH on Pt_{10} in neutral, anionic and cationic charge states

Properties	**Pt_{10} / H**			**Pt_{10} / OH**		
	Cationic	Neutral	Anionic	Cationic	Neutral	Anionic
E_{ads} (a.u.)	-0.1139	-0.1145	-0.0904	-0.0993	-0.1025	-0.0893
d_{av} (Å)	2.3945	2.4066	2.4100	2.2993	2.3100	2.3120
$d_{adsorbate\text{-}Pt}$ (Å)	1.7601	1.5975	1.6072	1.9476	1.9729	1.9691
ECN	3.3635	3.3840	3.3553	3.5901	3.6103	3.5659
υ (cm^{-1})	1388	2056	2018	3642	3657	3666

E_{ad}, calculated adsorption energy; d_{av}, calculated average weighted bond length; $d_{adsorbate\text{-}Pt}$, equilibrium bond length between H and OH with Pt; ECN, effective coordination number in the cluster; υ is the vibrational frequencies of the adsorbed molecule with Pt.

Although the adsorption energies of OH do not show significant difference for all charge states, energetically more favorable adsorption state for Pt-OH system was obtained in the neutral charge state. Similarly, adsorption energy of hydrogen on Pt was found as a minimum where the system was in the neutral state. In the neutral state, hydrogen adsorption on the top of Pt cluster was the most favorable compared to OH and its adsorption energy is about -0.11 a.u. Equilibrium bond length between H and Pt was reached in the neutral state as 1.5975 Å while between OH and Pt was 1.9729 Å. Vibrational frequencies of the H atom reduces when there is a shifting from neutral state. Thus, adding one electron or remove on Pt cluster causes to decrease in vibrational frequencies. This behavior is not acceptable for OH adsorption since we found no remarkable shifting in the vibrational frequencies. We also obtained larger vibrational frequency when OH adsorbed on Pt_{10} than H adsorbed.

4.10.1.2. Adsorption Properties of H atom on Pt_{10} Cluster on Different Sites

The interaction of Pt_{10} cluster with hydrogen atom was investigated at DFT level using Gaussian 09. Calculations were performed using B3PW91 functional and LANL2DZ basis set with a spin unrestricted condition. Hydrogen atom was adsorbed from different sites such as top, bridge and hollow. Optimized structures of hydrogen atom on different sites of Pt_{10} cluster are shown in Figure 29.

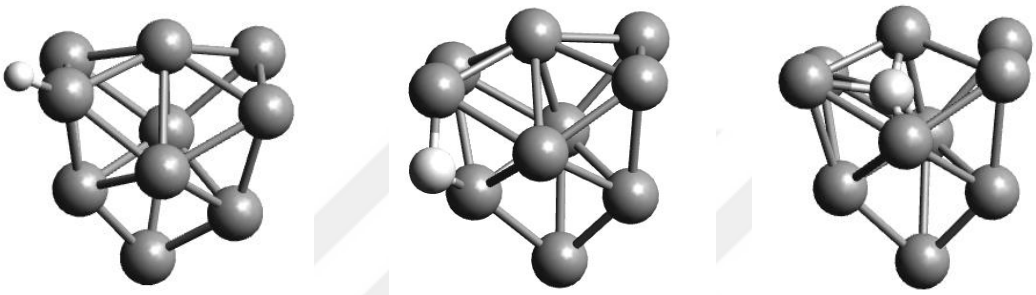

(a) Pt_{10}-H top (b) Pt_{10}-H bridge (c) Pt_{10}-H hollow

Figure 29. The lowest energy structures for the hydrogen adsorption on Pt_{10} cluster on different sites

In Table 10, we showed that the total energies and calculated adsorption energies for the hydrogen adsorption on P_{10} on top, bridge and hollow site.

Table 10. The total and adsorption energy of hydrogen on Pt_{10} cluster in top, bridge and hollow site

Energy (a.u)	**Pt_{10}-H top**	**Pt_{10}-H bridge**	**Pt_{10}-H hollow**
E_{tot}^{DFT}	-1193.4359	-1193.4340	-1193.4347
E_{ads}^{DFT}	-0.2169	-0.2149	-0.2157

The most favorable adsorption site for hydrogen on Pt_{10} cluster was obtained as top site. We also found the the bond length between H and the nearest Pt atom as 1.5758, 1.7806 and 1.6411 Å for top, bridge and hollow site respectively. This indicates that

where the lowest adsorption energy was reached, there was strong and close interaction between H and Pt atom.

4.10.2. Cu Cluster with H atom and OH Molecule

Global optimization of Cu_{10} cluster involving one hydrogen atom and OH molecule was done at DFT level using Gaussian 09.

4.10.2.1. Adsorption Properties of H and OH on Cu_{10} Cluster in Different Charge States

Figure 30 shows the ground state structures and total energies of Cu_{10} cluster with adsorbed hydrogen atom and OH molecule in the anionic, cationic and neutral charge states. Optimization were performed without freezing the structures.

From Figure 30, it can be seen that hydrogen atom preferred to bond at Cu-top in neutral state while Cu-bridge side in anionic and cationic charge state. In neutral and cationic charge states, the angle between H and the nearest two Cu atoms was obtained nearly as 90^0. In OH adsorption at different charge states, the angle between O and the nearest two Cu atoms was 80^0 and the angle of H-O-Cu system is 120^0. Moreover, adsorption energies and properties of Cu_{10} / H and Cu_{10} / OH systems are summarized in Table 11.

Energetically more favorable adsorption state for Cu-H system was obtained in the anionic charge state while cationic state for Cu-OH system. As also seen in Figure 30, there were no remarkable difference in total electronic energies for all charge states. Adsorption energy between OH and Cu was lower than H and Cu and this indicates that OH molecule can easily adsorbed on Cu atoms. Bond length between adsorbed species on Cu was found as the longest for Cu-H in the anionic state while the smallest for Cu-OH in the cationic state.

	Neutral $(Cu_{10}/H)^0$	**Anionic** $(Cu_{10}/H)^-$	**Cationic** $(Cu_{10}/H)^+$
Cu_{10} / H	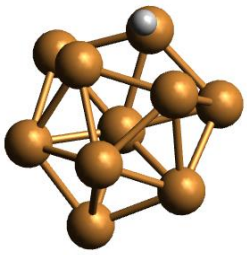	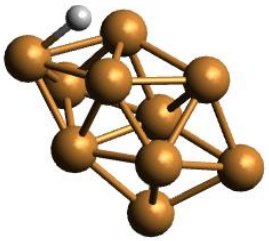	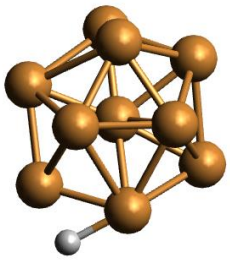
E_{tot} / a.u.	-1962.7935	-1962.8727	-1962.6023
	Neutral $(Cu_{10}/OH)^0$	**Anionic** $(Cu_{10}/OH)^-$	**Cationic** $(Cu_{10}/OH)^+$
Cu_{10} / OH	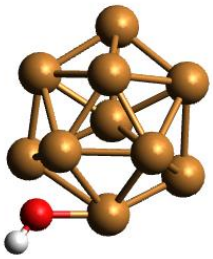	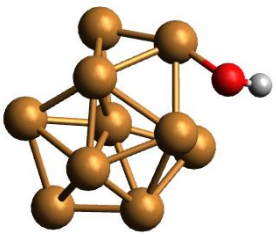	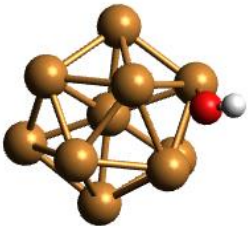
E_{tot} / a.u.	-2038.0482	-2038.0969	-2037.8508

Figure 30. The lowest energy structures and total energies of adsorbed H and OH on Cu_{10} cluster in neutral, anionic and cationic charge states (Cu is represented by yellow and hydrogen is by white while oxygen is represented by red)

Vibrational frequencies of the H atom on Cu_{10} reduces when the charge states change from cationic to anionic. This behavior is also true for OH adsorption on Cu_{10}. We also found larger vibrational frequency when OH adsorbed on Cu_{10} than H adsorbed which is an agreement with adsorption energies.

Table 11. Adsorption properties of H and OH on Cu_{10} in neutral, anionic and cationic charge states

Properties	Cu_{10} / H			Cu_{10} / OH		
	Cationic	Neutral	Anionic	Cationic	Neutral	Anionic
E_{ads} (a.u.)	-0.1013	-0.0914	-0.1109	-0.1472	-0.1436	-0.1325
d_{av} (Å)	2.3201	2.3423	2.2927	2.2376	2.2249	2.2212
$d_{adsorbate-Cu}$ (Å)	1.7148	1.7601	1.8466	2.0109	2.0149	1.9750
ECN	4.2813	4.1759	3.7974	4.3136	4.3575	4.0393
υ (cm^{-1})	1289	1160	1039	3757	3742	3737

E_{ad}, adsorption energy; d_{av}, calculated average weighted bond length; $d_{adsorbate-Cu}$, equilibrium bond length between H and OH with Cu; ECN, effective coordination number in the cluster; υ is the vibrational frequencies of the adsorbed molecule with Cu.

4.10.2.2. Adsorption Properties of H atom on Cu_{10} Cluster on Different Sites

The interaction of Cu_{10} cluster with hydrogen atom was investigated at DFT level using Gaussian 09. For DFT calculations, B3PW91 functional and LANL2DZ basis set with a spin unrestricted condition were used. Hydrogen atom was adsorbed from different sites as top, bridge and hollow. Optimized structures of hydrogen atom on different sites of Cu_{10} cluster are shown in Figure 31.

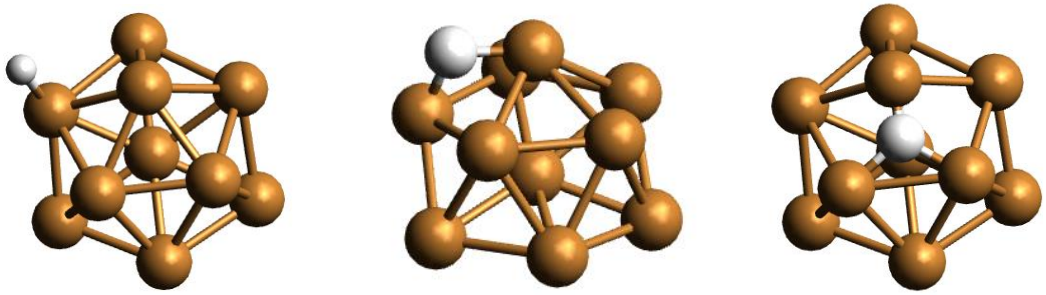

(a) Cu_{10}-H top (b) Cu_{10}-H bridge (c) Cu_{10}-H hollow

Figure 31. The lowest energy structures for the hydrogen adsorption on Cu_{10} cluster on different sites

In Table 12, we showed that the total energies and calculated adsorption energies for the hydrogen adsorption on Cu_{10} on top, bridge and hollow site.

Table 12. The total and adsorption energy of hydrogen on Cu_{10} cluster in top, bridge and hollow site

Energy (a.u)	**Cu_{10}-H top**	**Cu_{10}-H bridge**	**Cu_{10}-H hollow**
E_{tot}^{DFT}	-1963.3740	-1963.3741	-1963.3740
E_{ads}^{DFT}	-0.1709	-0.1711	-0.1709

The most favorable adsorption site for hydrogen on Cu_{10} cluster was obtained as bridge site. We also found the the bond length between H and the nearest Cu atom as 1.8113, 1.7677 and 1.8126 Å for top, bridge and hollow site respectively. This indicates that hydrogen adsorption from bridge site where the lowest adsorption energy was reached, there was strong interaction between H and Cu atom.

4.10.3. PtCu Cluster with H Atom and OH Molecule

Global optimization of Pt_3Cu_7 cluster involving one hydrogen atom and OH molecule separately was done at DFT level using Gaussian 09. Similarly with the previous, B3PW91 functional and LAN2DZ basis set was used with spin-unrestricted condition.

4.10.3.1. Adsorption Properties of H and OH on Pt_3Cu_7 Cluster in Different Charge States

In Figure 24, energetically most favorable composition was presented as Pt_3Cu_7 cluster since the minimum excess energy was found. In this part, global optimization of Pt_3Cu_7 with one hydrogen atom and OH molecule was done at DFT level using Gaussian 09. Figure 32 shows the ground state structures and total energies of Pt_3Cu_7 cluster with H and OH molecule in the anionic, cationic and neutral charge states.

	Neutral $(Pt_3Cu_7/H)^0$	**Anionic** $(Pt_3Cu_7/H)^-$	**Cationic** $(Pt_3Cu_7/H)^+$
Pt_3Cu_7 / H	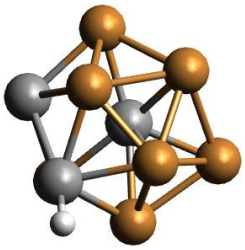	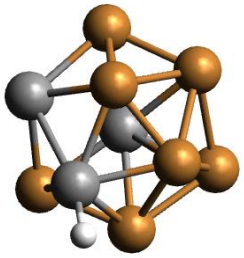	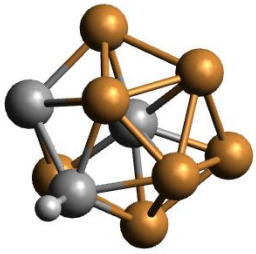
E_{tot} / a.u.	-1731.9763	-1731.9126	-1731.6843
	Neutral $(Pt_3Cu_7/OH)^0$	**Anionic** $(Pt_3Cu_7/OH)^-$	**Cationic** $(Pt_3Cu_7/OH)^+$
Pt_3Cu_7/ OH	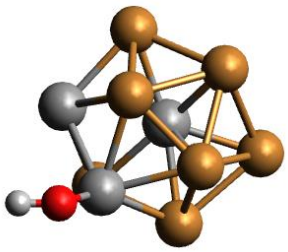	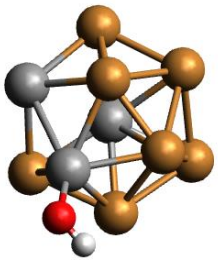	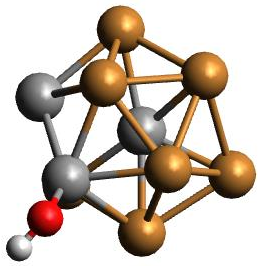
E_{tot} / a.u.	-1807.1716	-1807.0901	-1806.8828

Figure 32. The lowest energy structures and total energies of adsorbed H and OH on Pt_3Cu_7 cluster in neutral, anionic and cationic charge states

As seen in Figure 32, the lowest energy structure of Pt_3Cu_7 with H atom was obtained in the neutral state. Again, the lowest energy structure was found for Pt_3Cu_7-OH system in the neutral state. In neutral and cationic charge states, the angle of Pt-O-H bond was obtained as 115^0 while for anionic state as 110^0. Moreover, adsorption energies and adsorption properties of Pt_3Cu_7/ H and Pt_3Cu_7/ OH systems are summarized in Table 13.

Energetically more favorable adsorption state was obtained in the neutral charge state for Pt_3Cu_7-H system. Average bond length in the neutral state was calculated as 2.4116 Å which is the longest compared to other states.

Table 13. Adsorption properties of H and OH on Pt_3Cu_7 in the neutral, anionic and cationic charge states

Properties	Pt_3Cu_7 / H			Pt_3Cu_7 / OH		
	Cationic	Neutral	Anionic	Cationic	Neutral	Anionic
E_{ads} (a.u.)	-0.1134	-0.1167	-0.1059	-0.1094	-0.0914	-0.0987
d_{av} (Å)	2.3940	2.4116	2.3348	2.3146	2.2903	2.3022
$d_{adsorbate-Pt}$ (Å)	1.5703	1.5763	1.5905	1.9405	1.9837	2.0199
ECN	4.4795	4.5893	4.4738	4.1693	4.4062	4.3765
υ (cm^{-1})	2191	2179	2091	3659	3669	3678

E_{ad}, adsorption energy; d_{av}, calculated average weighted bond length; $d_{adsorbate-Pt}$, equilibrium bond length between H and OH with Pt; ECN, effective coordination number in the cluster; υ is the vibrational frequencies of the adsorbed molecule with Pt

For Pt_3Cu_7-OH system, the lowest adsorption energy was found in the cationic state and the bond length in this state was calculated as 2.3146 Å which is again the longest bond length compared to anionic and neutral state. Vibrational frequencies of the H atom on Pt_3Cu_7 decreases when the charge states changes from cationic to anionic. In contrast, vibrational frequency increases from cationic to anionic for Pt_3Cu_7 - OH system.

4.10.3.2. Adsorption Properties of H atom on Pt_3Cu_7 Cluster on Different Sites

The interaction of Pt_3Cu_7 cluster with hydrogen atom was investigated at DFT level using Gaussian 09. Hydrogen atom was adsorbed from top, bridge and hollow sites of Pt and Cu atoms. Optimized structures of adsorbed hydrogen atom to Pt_3Cu_7 cluster from top, bridge and hollow site of Pt and Cu atoms are shown in Figure 33.

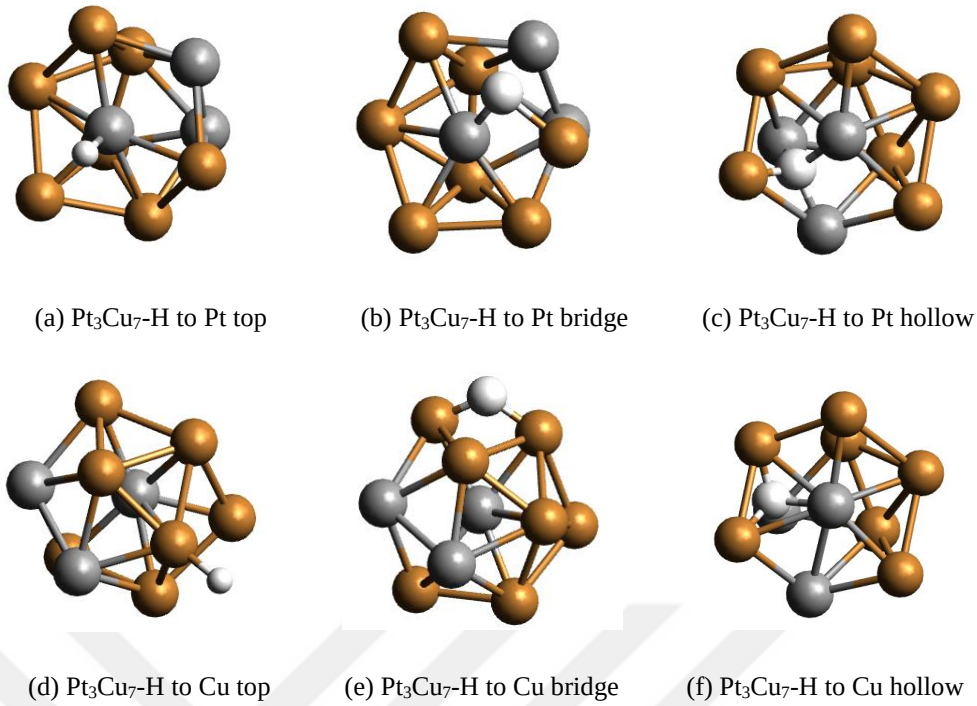

(a) Pt_3Cu_7-H to Pt top (b) Pt_3Cu_7-H to Pt bridge (c) Pt_3Cu_7-H to Pt hollow

(d) Pt_3Cu_7-H to Cu top (e) Pt_3Cu_7-H to Cu bridge (f) Pt_3Cu_7-H to Cu hollow

Figure 33. The lowest energy structures for the hydrogen adsorption on Cu_{10} cluster on different sites

In Table 14, we showed that the total energies and calculated adsorption energies for the hydrogen atom on Pt_3Cu_7 cluster from top, bridge and hollow site of Pt and Cu atoms.

Table 14. The total and adsorption energy of hydrogen Pt_3Cu_7 cluster from top, bridge and hollow site of Pt and Cu atoms.

Energy (a.u)	**Pt_3Cu_7-H to Pt top**	**Pt_3Cu_7-H to Pt bridge**	**Pt_3Cu_7-H to Pt hollow**
E_{tot}^{DFT}	-1732.5041	-1732.4946	-1732.5051
E_{ads}^{DFT}	-0.2069	-0.1974	-0.2079
	Pt_3Cu_7-H to Cu top	**Pt_3Cu_7-H to Cu bridge**	**Pt_3Cu_7-H to Cu hollow**
E_{tot}^{DFT}	-1731.2951	-1732.4587	-1732.4853
E_{ads}^{DFT}	-0.1708	-0.1615	-0.1881

The energetically most favorable adsorption site of hydrogen which bond from Pt site to the Pt_3Cu_7 cluster was found as hollow site. For hydrogen adsorption from Cu site to the Pt_3Cu_7 cluster, the most favorable adsorption site was also found hollow site. As seen in Table 14, the lowest adsorption energy was obtained on the Pt-hollow site as 0.2079 a.u. This also indicates that the hydrogen atom preferred to be bound to Pt atoms rather than Cu atoms. The bond length of Pt-H on hollow site was 1.5837 Å whereas Cu-H on hollow site was 1.6602 Å.

5. CONCLUSION

A detailed study on the lowest energy morphologies for Pt, Cu and PtCu clusters composed of 2-40 atoms was carried out using GA coupled with Gupta semi-empirical potential. As a searching strategy for the lowest energy structures, first 100 GA runs were carried out for all Pt, Cu and PtCu clusters and then the number of GA runs were extended up to 400. The lowest energy structures of pure Pt and Cu clusters composed of 2-40 atoms were successfully captured in 100 GA runs. Although the lowest energy structures were found for Pt and Cu composed of 20-40 atoms in 100 GA runs, the percentage of runs which gave the lowest energy structures increased when 200 GA runs were carried out.

For PtCu clusters composed of 2-20 atoms, 100 GA runs were found as a sufficient strategy to reach global minima (presumed). However, 100 GA runs remained incapable to find lowest energy structures for clusters above 20 atoms and caused clusters to set in one of the local minima. Potential energy results indicate that 400 GA runs is a good strategy to find global minima for PtCu clusters contained more than 20 atoms.

After the lowest energy structures of Pt, Cu and PtCu clusters composed of 2-40 atoms were found, several energetic quantities such as binding, excess and second difference in energy were calculated to evaluate stabilities of each cluster. The results showed that optimized clusters were energetically favorable since they had positive binding and second difference in energy and negative excess energy values. Structural analysis showed that Pt clusters were based on icosahedron and closed packed fcc-like TO for Pt_{38}. Layered morphology was found as a global minima for Pt_{40} whereas distorted icosahedron structure was confirmed to be less favored. For Cu clusters, icosahedral growth was observed after 18 atoms. Mackay-like structures were found for larger sizes which was consistent with Darby et al.'s work [48]. Similarly with 38 atoms of Pt, perfect

TO were obtained as a global minima. Also, the lowest energy structures of both Cu and Pt clusters were highly symmetric and ordered. PtCu clusters were mainly based on distorted icosahedron and no symmetric morphology can be seen after 30 atoms. In all sizes of PtCu clusters, Pt segregated in core region while Cu atoms tended to segregate to the surface. Cu atoms preferred to bond to Pt atoms rather than Cu atoms due to the strong binding energy of Pt atoms. Second order parameters showed that optimum structures for PtCu clusters consisting of 2-40 atoms were not homogeneously mixed.

To obtain better understanding on adsorption properties of clusters, hydrogen and OH adsorption on small size of pure Pt, Cu and PtCu clusters in different charge states (neutral, anionic and cationic) and in different sites (top, bridge and hollow) was studied. Structure optimization with H and OH adsorbed clusters were performed within DFT approach using Gaussian 09. Our results showed that the lowest energy structure was obtained for both H and OH on Pt_3Cu_7 cluster in the neutral state. Stretching between H and Pt atoms decreased from cationic to anionic whereas increased for OH and Pt stretching. For adsorption site preference, we found that H atoms are preferentially bound to the Pt atoms from hollow site. Although hydrogen can bind to Cu-hollow in bimetallic PtCu, clusters, lower adsorption energy was achieved with H to Pt (hollow) formation.

REFERENCES

1. The MathWorks, I., Natisk, Massachusetts, United States, *MATLAB 2014a*. 2014.
2. Gumina, G., et al., *gamma-Fe2O3 nanoparticle surface controls PtFe nanoparticle growth and catalytic properties.* Nanoscale, 2013. **5**(7): p. 2921-2927.
3. Kim, J., Y. Lee, and S.H. Sun, *Structurally Ordered FePt Nanoparticles and Their Enhanced Catalysis for Oxygen Reduction Reaction.* Journal of the American Chemical Society, 2010. **132**(14): p. 4996-4997.
4. Piotrowski, M.J., P. Piquini, and J.L.F. Da Silva, *Platinum-Based Nanoalloys PtnTM55-n (TM=Co, Rh, Au): A Density Functional Theory Investigation.* Journal of Physical Chemistry C, 2012. **116**(34): p. 18432-18439.
5. Rossi, G., R. Ferrando, and C. Mottet, *Structure and chemical ordering in CoPt nanoalloys.* Faraday Discussions, 2008. **138**: p. 193-210.
6. Yu, Z.Q., et al., *Comparison between Dealloyed PtCo3 and PtCu3 Cathode Catalysts for Proton Exchange Membrane Fuel Cells.* Journal of Physical Chemistry C, 2012. **116**(37): p. 19877-19885.
7. Gan, L., et al., *Core-Shell Compositional Fine Structures of Dealloyed PtxNi1-x Nanoparticles and Their Impact on Oxygen Reduction Catalysis.* Nano Letters, 2012. **12**(10): p. 5423-5430.
8. Ghosh, T., et al., *Pt Alloy and Intermetallic Phases with V, Cr, Mn, Ni, and Cu: Synthesis As Nanomaterials and Possible Applications As Fuel Cell Catalysts.* Chemistry of Materials, 2010. **22**(7): p. 2190-2202.
9. Zhao, Y., et al., *A new route for the electrodeposition of platinum-nickel alloy nanoparticles on multi-walled carbon nanotubes.* Electrochimica Acta, 2007. **52**(19): p. 5873-5878.
10. Sarkar, A. and A. Manthiram, *Synthesis of Pt@Cu Core-Shell Nanoparticles by Galvanic Displacement of Cu by Pt4+ Ions and Their Application as Electrocatalysts for Oxygen Reduction Reaction in Fuel Cells.* Journal of Physical Chemistry C, 2010. **114**(10): p. 4725-4732.
11. Yang, H.Z., et al., *Electrooxidation of methanol and formic acid on PtCu nanoparticles.* Electrochimica Acta, 2010. **55**(27): p. 8000-8004.
12. Yeh, T.H., et al., *Preparation of carbon-supported PtM (M = Au, Pd, or Cu) nanorods and their application in oxygen reduction reaction.* Electrochemistry Communications, 2013. **31**: p. 125-128.
13. Zhou, S.H., et al., *Pt-Cu core-shell and alloy nanoparticles for heterogeneous NOx, reduction: Anomalous stability and reactivity of a core-shell nanostructure.* Angewandte Chemie-International Edition, 2005. **44**(29): p. 4539-4543.
14. Kang, Y.J., et al., *Synthesis, Shape Control, and Methanol Electro-oxidation Properties of Pt-Zn Alloy and Pt3Zn Intermetallic Nanocrystals.* Acs Nano, 2012. **6**(6): p. 5642-5647.
15. Miura, A., et al., *Synthesis of Intermetallic PtZn Nanoparticles by Reaction of Pt Nanoparticles with Zn Vapor and Their Application as Fuel Cell Catalysts.* Chemistry of Materials, 2009. **21**(13): p. 2661-2667.
16. Oezaslan, M.H., F.; Strasser, P., *Pt-Based Core-Shell Catalyst Architectures for Oxygen Fuel Cell Electrodes.* Journal of Physical Chemistry Letters, 2013. **4**(19): p. 3273-3291.
17. Stephens, I.E.L., et al., *Understanding the electrocatalysis of oxygen reduction on platinum and its alloys.* Energy & Environmental Science, 2012. **5**(5): p. 6744-6762.

18. Braunchweig, B., et al., *Electrocatalysis: A direct alcohol fuel cell and surface science perspective.* Catalysis Today, 2013. **202**: p. 197-209.
19. Long, N.V., et al., *The development of mixture, alloy, and core-shell nanocatalysts with nanomaterial supports for energy conversion in low-temperature fuel cells.* Nano Energy, 2013. **2**(5): p. 636-676.
20. Ferrando, R., J. Jellinek, and R.L. Johnston, *Nanoalloys: From theory to applications of alloy clusters and nanoparticles.* Chemical Reviews, 2008. **108**(3): p. 845-910.
21. Chaves, A.S., et al., *Structural formation of binary PtCu clusters: A density functional theory investigation.* Computational Materials Science, 2015. **98**: p. 278-286.
22. Lipkowski, J. and P.N. Ross, *Imaging of surfaces and interfaces*. 1999: Wiley-VCH.
23. Schmid, G. and D. Fenske, *Metal clusters and nanoparticles INTRODUCTION.* Philosophical Transactions of the Royal Society a-Mathematical Physical and Engineering Sciences, 2010. **368**(1915): p. 1207-1210.
24. Mathew, A. and T. Pradeep, *Noble Metal Clusters: Applications in Energy, Environment, and Biology.* Particle & Particle Systems Characterization, 2014. **31**(10): p. 1017-1053.
25. Molenbroek, A.M., S. Haukka, and B.S. Clausen, *Alloying in Cu/Pd nanoparticle catalysts.* Journal of Physical Chemistry B, 1998. **102**(52): p. 10680-10689.
26. Heiles, S. and R.L. Johnston, *Global optimization of clusters using electronic structure methods.* International Journal of Quantum Chemistry, 2013. **113**(18): p. 2091-2109.
27. Deheer, W.A., *THE PHYSICS OF SIMPLE METAL-CLUSTERS - EXPERIMENTAL ASPECTS AND SIMPLE-MODELS.* Reviews of Modern Physics, 1993. **65**(3): p. 611-676.
28. Cohen, A.J., P. Mori-Sanchez, and W.T. Yang, *Challenges for Density Functional Theory.* Chemical Reviews, 2012. **112**(1): p. 289-320.
29. Perdew, J.P. and A. Ruzsinszky, *Fourteen Easy Lessons in Density Functional Theory.* International Journal of Quantum Chemistry, 2010. **110**(15): p. 2801-2807.
30. R. G. Parr, W.Y., *Density Functional Theory of Atoms and Molecules*. 1989: Oxford University Press.
31. Rossi, G., et al., *Global optimization of bimetallic cluster structures. II. Size-matched Ag-Pd, Ag-Au, and Pd-Pt systems.* Journal of Chemical Physics, 2005. **122**(19).
32. Jones, J.E., *On the Determination of Molecular Fields. II. From the Equation of State of a Gas.* Proceedings of the Royal Society of London. Series A, 1924. **106**(738): p. 463-477.
33. Sutton, A.P. and J. Chen, *LONG-RANGE FINNIS SINCLAIR POTENTIALS.* Philosophical Magazine Letters, 1990. **61**(3): p. 139-146.
34. Born, M. and J.E. Mayer, *Zur Gittertheorie der Ionenkristalle.* Zeitschrift für Physik, 1932. **75**(1): p. 1-18.
35. Cleri, F. and V. Rosato, *Tight-binding potentials for transition metals and alloys.* Physical Review B, 1993. **48**(1): p. 22-33.
36. Gupta, R.P., *Lattice relaxation at a metal surface.* Physical Review B, 1981. **23**(12).
37. Rosato, V., M. Guillope, and B. Legrand, *THERMODYNAMICAL AND STRUCTURAL-PROPERTIES OF FCC TRANSITION-METALS USING A SIMPLE TIGHT-BINDING MODEL.* Philosophical Magazine a-Physics of

Condensed Matter Structure Defects and Mechanical Properties, 1989. **59**(2): p. 321-336.
38. Booker, L.B. and R. Riolo, *Introduction to the Special Issue: Advances in Genetic Algorithms - Research Trends and Perspectives.* Evolutionary Computation, 2000. **8**(4): p. III-IV.
39. Roberts, C., R.L. Johnston, and N.T. Wilson, *A genetic algorithm for the structural optimization of Morse clusters.* Theoretical Chemistry Accounts, 2000. **104**(2): p. 123-130.
40. Wolf, M.D. and U. Landman, *Genetic algorithms for structural cluster optimization.* Journal of Physical Chemistry A, 1998. **102**(30): p. 6129-6137.
41. Becker, E.W., K. Bier, and W. Henkes, *Strahlen aus kondensierten Atomen und Molekeln im Hochvakuum.* Zeitschrift für Physik, 1956. **146**(3): p. 333-338.
42. Nesselberger, M., et al., *The effect of particle proximity on the oxygen reduction rate of size-selected platinum clusters.* Nat Mater, 2013. **12**(10): p. 919-924.
43. Liao, P.C., et al., *CO oxidation activity and XPS studies of Pt・Cuγ-Al2O3 bimetallic catalysts.* Journal of Catalysis, 1982. **74**(2): p. 307-316.
44. Fornasari, G., et al., *Novel low temperature NOx storage-reduction catalysts for diesel light-duty engine emissions based on hydrotalcite compounds.* Catalysis Today, 2002. **75**(1): p. 421-429.
45. de Jongste, H.C., V. Ponec, and F.G. Gault, *Influence of alloying Pt with Cu on the reaction mechanisms of hydrocarbon reforming reactions.* Journal of Catalysis, 1980. **63**(2): p. 395-403.
46. Mani, P., R. Srivastava, and P. Strasser, *Dealloyed Pt−Cu Core−Shell Nanoparticle Electrocatalysts for Use in PEM Fuel Cell Cathodes.* The Journal of Physical Chemistry C, 2008. **112**(7): p. 2770-2778.
47. Dutta, I., et al., *Electrochemical and Structural Study of a Chemically Dealloyed PtCu Oxygen Reduction Catalyst.* The Journal of Physical Chemistry C, 2010. **114**(39): p. 16309-16320.
48. Darby, S., et al., *Theoretical study of Cu-Au nanoalloy clusters using a genetic algorithm.* Journal of Chemical Physics, 2002. **116**(4): p. 1536-1550.
49. Guedes-Sobrinho, D., et al., *Structure, Electronic, and Magnetic Properties of Binary PtnTM55–n (TM = Fe, Co, Ni, Cu, Zn) Nanoclusters: A Density Functional Theory Investigation.* The Journal of Physical Chemistry C, 2015. **119**(27): p. 15669-15679.
50. Born, M. and R. Oppenheimer, *Zur Quantentheorie der Molekeln.* Annalen der Physik, 1927. **389**(20): p. 457-484.
51. Ferrando, R., *Global Optimization of Free and Supported Clusters*, in *Metal Clusters and Nanoalloys: From Modeling to Applications*. 2013, Springer New York: New York, NY. p. 195-214.
52. Buff, F.P., *The Spherical Interface. I. Thermodynamics.* The Journal of Chemical Physics, 1951. **19**(12): p. 1591-1594.
53. Oxtoby, D.W., *Nucleation of first-order phase transitions.* Accounts of Chemical Research, 1998. **31**(2): p. 91-97.
54. Schrödinger, E., *Quantisierung als Eigenwertproblem.* Annalen der Physik, 1926. **384**(4): p. 361-376.
55. Feynman, R.P., N. Metropolis, and E. Teller, *Equations of State of Elements Based on the Generalized Fermi-Thomas Theory.* Physical Review, 1949. **75**(10): p. 1561-1573.
56. Hohenberg, P. and W. Kohn, *Inhomogeneous Electron Gas.* Physical Review, 1964. **136**(3B): p. B864-B871.

57. Kohn, W. and L.J. Sham, *Self-Consistent Equations Including Exchange and Correlation Effects.* Physical Review, 1965. **140**(4A): p. A1133-A1138.
58. Lieb, E.H. and B. Simon, *The Thomas-Fermi theory of atoms, molecules and solids.* Advances in Mathematics, 1977. **23**(1): p. 22-116.
59. Levy, M., *Universal variational functionals of electron densities, first-order density matrices, and natural spin-orbitals and solution of the v-representability problem.* Proceedings of the National Academy of Sciences, 1979. **76**(12): p. 6062-6065.
60. Kohn, W., *Electronic structure of matter: Wave functions and density functionals.* Chimia, 2000. **54**(1-2): p. 50-50.
61. Ferrando, R., A. Fortunelli, and G. Rossi, *Quantum effects on the structure of pure and binary metallic nanoclusters.* Physical Review B, 2005. **72**(8).
62. Paz-Borbon, L.O., A. Gupta, and R.L. Johnston, *Dependence of the structures and chemical ordering of Pd-Pt nanoalloys on potential parameters.* Journal of Materials Chemistry, 2008. **18**(35): p. 4154-4164.
63. Bonacickoutecky, V., P. Fantucci, and J. Koutecky, *QUANTUM-CHEMISTRY OF SMALL CLUSTERS OF ELEMENTS OF GROUP-IA, GROUP-IB, AND GROUP-IIA - FUNDAMENTAL-CONCEPTS, PREDICTIONS, AND INTERPRETATION OF EXPERIMENTS.* Chemical Reviews, 1991. **91**(5): p. 1035-1108.
64. Calvo, F. and E. Yurtsever, *Mapping the global minima of binary Morse clusters: The effects of range mismatch.* Computational and Theoretical Chemistry, 2013. **1021**: p. 7-15.
65. Stukowski, A., *Structure identification methods for atomistic simulations of crystalline materials.* Modelling and Simulation in Materials Science and Engineering, 2012. **20**(4).
66. Hoppe, R., *Effective coordination numbers (ECoN) and mean fictive ionic radii (MEFIR)*, in *Zeitschrift für Kristallographie - Crystalline Materials*. 1979. p. 23.
67. Da Silva, J.L.F., *Effective coordination concept applied for phase change (GeTe)(m)(Sb2Te3)(n) compounds.* Journal of Applied Physics, 2011. **109**(2).
68. Hoppe, R., et al., *A NEW ROUTE TO CHARGE-DISTRIBUTIONS IN IONIC SOLIDS.* Journal of the Less-Common Metals, 1989. **156**: p. 105-122.
69. Ducastelle, F., *Order and phase stability in alloys*, in *Cohesion and Structures*. 1991: North-Holland, Amsterdam.
70. Guedes-Sobrinho, D., et al., *Structure, Electronic, and Magnetic Properties of Binary PtnTM55-n (TM = Fe, Co, Ni, Cu, Zn) Nanoclusters: A Density Functional Theory Investigation.* Journal of Physical Chemistry C, 2015. **119**(27): p. 15669-15679.
71. Wales, D.J. and J.P.K. Doye, *Global Optimization by Basin-Hopping and the Lowest Energy Structures of Lennard-Jones Clusters Containing up to 110 Atoms.* The Journal of Physical Chemistry A, 1997. **101**(28): p. 5111-5116.
72. Johnston, R.L., *Evolving better nanoparticles: Genetic algorithms for optimising cluster geometries.* Dalton Transactions, 2003(22): p. 4193-4207.
73. Marcelo Mario Mariscal, O.A.O., Ezequiel Pedro Marcos Leiva, *Metal Clusters and Nanoalloys: From Modeling to Applications*. 1 ed. Nanostructure Science and Technology. 2013: Springer-Verlag New York.
74. Hartke, B., *Application of Evolutionary Algorithms to Global Cluster Geometry Optimization*, in *Applications of Evolutionary Computation in Chemistry*, R.L. Johnston, Editor. 2004, Springer Berlin Heidelberg: Berlin, Heidelberg. p. 33-53.

75. Hanwell, M.D., et al., *Avogadro: an advanced semantic chemical editor, visualization, and analysis platform.* Journal of Cheminformatics, 2012. **4**(1): p. 17.
76. M. J. Frisch, G.W.T., H. B. Schlegel, G. E. Scuseria, , et al., *Gaussian 09*. 2013, Gaussian, Inc., Wallingford CT.
77. Becke, A.D., *Density-functional exchange-energy approximation with correct asymptotic behavior.* Physical Review A, 1988. **38**(6): p. 3098-3100.
78. Perdew, J.P., et al., *Atoms, molecules, solids, and surfaces: Applications of the generalized gradient approximation for exchange and correlation.* Physical Review B, 1992. **46**(11): p. 6671-6687.
79. Massen, C., T.V. Mortimer-Jones, and R.L. Johnston, *Geometries and segregation properties of platinum-palladium nanoalloy clusters.* Journal of the Chemical Society-Dalton Transactions, 2002(23): p. 4375-4388.
80. Tran, D.T. and R.L. Johnston, *Study of 40-atom Pt-Au clusters using a combined empirical potential-density functional approach.* Proceedings of the Royal Society a-Mathematical Physical and Engineering Sciences, 2011. **467**(2131): p. 2004-2019.
81. Boyukata, M. and J.C. Belchior, *Structural and energetic analysis of copper clusters: MD study of Cu-n (n=2-45).* Journal of the Brazilian Chemical Society, 2008. **19**(5): p. 884-893.
82. Hanwell, M.D., et al., *Avogadro: an advanced semantic chemical editor, visualization, and analysis platform.* Journal of Cheminformatics, 2012. **4**.
83. Mani, P., R. Srivastava, and P. Strasser, *Dealloyed Pt-Cu core-shell nanoparticle electrocatalysts for use in PEM fuel cell cathodes.* Journal of Physical Chemistry C, 2008. **112**(7): p. 2770-2778.

APPENDIX

MATLAB Code for GA Operators:

```
% %INITIALIZATION OF CLUSTERS
for i=1:Npop
    i
    names(i)=initial_c(N,type1,type2,r_type1,r_type2);
end

names_init=names;

%%%%%%%%%%%%%%%%%%%%%%%%%%%%%%%%%%%%%%%%%%%%%%%%%%%%%%%%%%%%
%%%%%%%%%%%%%%%%
%   ITERATION STARTS
%%%%%%%%%%%%%%%%%%%%%%%%%%%%%%%%%%%%%%%%%%%%%%%%%%%%%%%%%%%%
%%%%%%%%%%%%%%%%

for ii=1:Niter
    names_old=names;
    for i=1:Npop
        coor=cell2mat(names(i));
        Vcluster(i,2)=guptapotential(N,A,coor);
        Vcluster(i,1)=i;
        Names(i)=coor;
    end

%CALCULATION OF FITNESS VALUES
    Vmax=max(Vcluster(:,2));
    Vmin=min(Vcluster(:,2));

Vcluster(:,3)=fittingfunction(alpha,Vcluster,Vmin,Vmax,Npop
);

%SORTING WRT POTENTIAL
    Vcluster=sortrows(Vcluster,2);

%CLUSTERS THAT ARE KEPT FOR NEXT RUN
    for i=1:Ngen
        k=Vcluster(i,1);
        names_new(i)=names(k);
    end

%SELECTION OF MATES
    [male,female]=mating(Npop,Nmat,Vcluster(:,3),names);

%CROSSOVER FOR SINGLE ELEMENT CLUSTERS
    if or(type2==0,type1==0)
        for i=1:Nmat
            coor=cell2mat(male(i));
            male1=transformation_xy(coor);
            male1=sortrows(male(i),2+mod(ii,3));
            coor=cell2mat(female(i));
            female1=transformation_xy(coor);
```

```
            female1=sortrows(female(i),2+mod(ii,3));

names_new(i+Ngen)=[male1(1:M,:);female1(M+1:N,:)];
            coor=cell2mat(names_new(ii+Ngen));
            Af=swap_mut(ii,coor);
            names_new(i+Ngen)=Af;
        end
    else

%CROSSOVER FOR DOUBLE ELEMENTS CLUSTERS
        for i=1:Nmat
            coor=cell2mat(male(i));
            male1=transformation_xy(coor);
            coor=cell2mat(female(i));
            female1=transformation_xy(coor);
            male1=sortrows(male(i),2+mod(ii,3));
            female1=sortrows(female(i),2+mod(ii,3));
            male1a=male1(1:M,:);
            counter=sum(male1a(:,1));
            type2_male=counter-floor(N/2);
            type1_male=floor(N/2)-type2_male;
            type1_female=type1-type1_male;
            type2_female=type2-type2_male;
            counter1=0;
            counter2=0;
            k=0;
            female1a=[];
            for j=1:N
                if female1(N+1-j,1)==1
                    if counter1<type1_female;
                        k=k+1;
                        counter1=counter1+1;
                        female1a(k,:)=female1(N+1-j,:);
                        sum(female1a(:,1));
                    end
                else
                    if counter2<type2_female
                        k=k+1;
                        counter2=counter2+1;
                        female1a(k,:)=female1(N+1-j,:);
                        sum(female1a(:,1));
                    end
                end
            end
            names_new(i+Ngen)=[male1a(1:M,:);female1a(1:N-
M,:)];
            coor=cell2mat(names_new(i+Ngen));
            Af=swap_mut(ii,coor);
            names_new(i+Ngen)=Af;
        end
    end
```

```
%MUTATION --- SWAPING ATOMS OF DIFFERENT TYPES (FASTER
CONVERGENCE IF HETEOROATOMS > 10 EXIST
    if mut_type==1     % (swapping the atoms)
        for l=1:Nmut
           k=randi(Npop);
           coor=cell2mat(names_new(k));
           for j=1:floor(N/6)
               n=randi(N);
               m=randi(N);
               while coor(m,1)==coor(n,1)
                   m=randi(N);
               end
               coor([n m],1) = coor([m n],1);
           end

           Af=swap_mut(ii,coor);
           names_new(k)=Af;
        end
    else
        for l=1:Nmut
           k=randi(Npop-Ngen);
           k=k+Ngen;
           coor=cell2mat(names_old(k));
           mut1=coor(1:floor(N/2),:);
           mut2=coor(floor(N/2)+1:N,:);
           mut1=transformation_xy(mut1);
           coor=[mut1;mut2];
           Af=swap_mut(ii,coor);
           names_old(k)=Af;
        end
    end

%NATURAL SELECTION
        names=names_new;
        new_ones=[names_old names_new(Ngen+1:Npop)];
        for i=1:Npop+Nmat
            coor=cell2mat(new_ones(i));
            Vnew(i,2)=guptapotential(N,A,coor);
            Vnew(i,1)=i;
        End

%SORTING WRT POTENTIAL
    Vnew=sortrows(Vnew,2);


%CLUSTERS THAT ARE KEPT FOR NEXT RUN
    for i=1:Npop
        k=Vnew(i,1);
        names_new(i)=new_ones(k);
    end
```

```
    names=names_new;
    ii
    Vnew%(1:15,:)
    if abs(Vnew(Npop,2)-Vnew(1,2))<1e-5
        break
    end
end
names(1)
Vcluster(1,:)


%AN OUTPUT FILE ('celldata.com') IS CREATED FOR GAUSSVIEW
coor=cell2mat(names_new(1));
for i=1:N
    if coor(i,1)==1
        C(i,1)=atom1;
    else
        C(i,1)=atom2;
    end
    C(i,2)=coor(i,2);
    C(i,3)=coor(i,3);
    C(i,4)=coor(i,4);
end


%output file for Gauss-View
fileID = fopen('celldata.com','wt');
fprintf(fileID,'%s \n','%chk=au10cu1022nd.chk');
fprintf(fileID,'%s \n','# opt freq b3pw91/lanl2mb
geom=connectivity');
fprintf(fileID,'%s \n','');
fprintf(fileID,'%s \n','Title Card');
fprintf(fileID,'%s \n','');
fprintf(fileID,'%d %d \n',0, 3);
formatSpec = '%s %7.4f %7.4f %7.4f \n';
[nrows,ncols] = size(C);
for row = 1:nrows
    fprintf(fileID,formatSpec,C{row,:}));
end
fclose(fileID);

save(['N',num2str(N),'_Pt',num2str(type2),'_Cu',num2str(typ
e1),'iteration',num2str(iter),'.mat'])

end
```

MATLAB Code for ECN Concept:

```
clear all
clc
```

```
iijk=0;
%coor=[1 0 1 1; 1 0 0 3];
%N=2;
for iij=2:2:40
    iijk=iijk+1;
    load(['file directory','N', num2str (iij),
'_Pt',num2str(iij/2),'_Cu',num2str(iij/2),'.mat'])

    d_coor=coor(:,2:4);
    for i=1:N
        l=0;
        for k=1:N
            d(i,k)=((d_coor(i,1)-
d_coor(k,1))^2+(d_coor(i,2)-d_coor(k,2))^2+(d_coor(i,3)-
d_coor(k,3))^2)^0.5;
            if d(i,k)~=0
                l=l+1;
                dnew(i,l)=d(i,k);
            end
        end
        davt=mean(dnew(i,:));
        da(i)=fminsearch(@(dav_o)
avg_d1(i,N,d,dav_o),davt);
        danew(i)=fminsearch(@(dav_o) avg_d1(i,N
1,dnew,dav_o),davt);
    end

    for i=1:N
        ECN(i)=0;
        for j=1:N
            ECN(i)=ECN(i)+exp(1-(d(i,j)/da(i))^6);
        end
    end
    N_11=0;
    N_22=0;
    N_12=0;
    for i=1:N
        for j=1:N
            if coor(i)==coor(j)
                if coor(i)==1
                    if d(i,j)<2.75
                        N_11=N_11+1;
                    end
                elseif coor(i)==2
                    if d(i,j)<2.62
                        N_11=N_11+1;
                    end
                end
            else
                if d(i,j)<2.80
                    N_12=N_12+1;
                end
```

```
            end
        end
    end


    sigma=(N_11+N_22-N_12)/(N_11+N_22+N_12);
    ECN_av=sum(ECN)/N;
    dav_avg=sum(da)/N;
    ECN_all(iijk,4)=sigma;
    ECN_all(iijk,3)=ECN_av;
    ECN_all(iijk,2)=dav_avg;
    ECN_all(iijk,1)=N;

end
ECN_all
```